Kirk-Othmer Encyclopedia of Chemical Technology.

THIN FILMS, MONOMOLECULAR LAYERS

Molecularly engineered materials can be fabricated from the molecular level up, and their physical properties can be both predicted and designed. Surface analytical tools enable investigations of monomolecular layers in previously unprecedented detail, leading to understanding of molecular packing and ordering. These tools also provide information to aid in understanding the relationships between the structure and properties of the individual molecule as well as of the material it forms (see Surface and interface analysis).

Supramolecular assemblies are fabricated by assembling molecules that interlock in a planned, hierarchical manner, forming structures having specific desired functions. There are two principal methods. Using the Langmuir-Blodgett technique, molecular layers are formed at air–water interfaces under programmed external influence. The different kinds of monolayers are superimposed in an intelligently planned sequence, forming increasingly more complex supramolecular structures. In the self-assembly technique, layers are formed spontaneously by molecules self-organizing at a solid–liquid interface, and multilayer structures are formed only after the monolayer surface has been chemically modified.

1. Langmuir-Blodgett Films

The discovery that monolayer films can be transferred from the air–water interface onto a solid substrate by a simple dipping technique (1) and the subsequent report that multilayers can be built up by sequential monolayer transfer (2) opened a significant new area in science to further investigation (3, 4). Studies of these multilayers led to a patent describing the use of Langmuir-Blodgett (LB) films for preparing nonreflecting glass (5).

Langmuir-Blodgett was the first technique to provide a practical route for the construction of ordered molecular assemblies. These monolayers, which provide design flexibility both at the individual molecular and at the material levels, are prepared at the water–air interface using a fully computerized trough (Fig. 1). Detailed discussions of troughs (4) and of surface pressure, π, and methods of surface pressure measurements are available (3, 6).

1.1. Monolayers at the Air–Water Interface

Molecules that form monolayers at the water–air interface are called amphiphiles or surfactants (qv). Such molecules are insoluble in water. One end is hydrophilic, and therefore is preferentially immersed in the water; the other end is hydrophobic, and preferentially resides in the air, or in a nonpolar solvent. A classic example of an amphiphile is stearic acid, $C_{17}H_{35}COOH$, wherein the long hydrocarbon tail, $C_{17}H_{35}$–, is hydrophobic, and the carboxylic acid group, –COOH, is hydrophilic. This carboxylic group can dissociate in water to give a negatively charged ion, COO^-. Complex organic amphiphiles containing chromophores, various donor or acceptor groups, etc, can be designed and synthesized. Understanding the structure of such monolayers can be assisted by computer modeling (4) (see Computer technology; Molecular modeling).

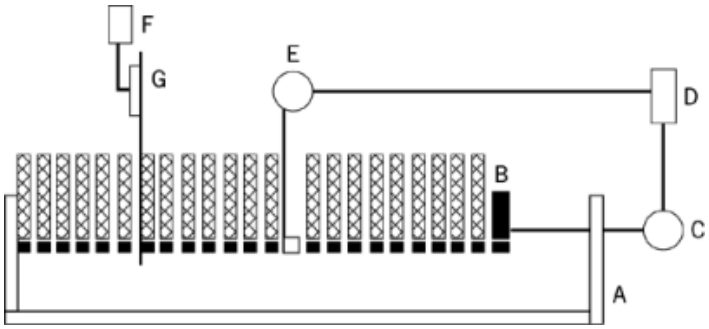

Fig. 1. A trough for deposition of monolayers on solid substrates: A, bath; B, a moving barrier; C, a motor; D, a pressure-control device; E, a surface pressure balance; F, a motor with a gearbox that lowers and raises the substrate; and G, a solid substrate. The film material (⊠) has a hydrophobic tail and (■) hydrophilic head.

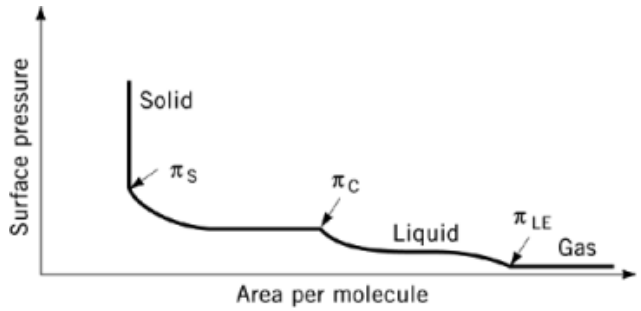

Fig. 2. A schematic π-A isotherm for a phospholipid of fatty acid (see text).

The monolayer resulting when amphiphilic molecules are introduced to the water–air interface was traditionally called a two-dimensional gas owing to what were the expected large distances between the molecules. However, it has become quite clear that amphiphiles self-organize at the air–water interface even at relatively low surface pressures (7–10). For example, x-ray diffraction data from a monolayer of heneicosanoic acid spread on a 0.5-mM $CaCl_2$ solution at zero pressure (11) showed that once the barrier starts moving and compresses the molecules, the surface pressure, π, increases and the area per molecule, A, decreases. The surface pressure, ie, the force per unit length of the barrier (in N/m) is the difference between σ_0, the surface tension of pure water, and σ, that of the water covered with a monolayer. Where the total number of molecules and the total area that the monolayer occupies is known, the area per molecules can be calculated and a π-A isotherm constructed. This isotherm (Fig. 2), which describes surface pressure as a function of the area per molecule (3, 4), is rich in information on stability of the monolayer at the water–air interface, the reorientation of molecules in the two-dimensional system, phase transitions, and conformational transformations.

As the barrier moves, the molecules are compressed, the intermolecular distance decreases, the surface pressure increases, and a phase transition may be observed in the isotherm. These phase transitions, characterized by a break in the isotherm, may vary with the subphase pH, and temperature. The first-phase transition, π_{LE} in Figure 2, is assigned to a transition from the gas to the liquid state, also known as the liquid-expanded, LE, state. In the liquid phase, the monolayer is more coherent and the molecules occupy a smaller area than in the gas phase, but have neither positional nor orientational order. The molecules have more degrees of freedom and gauche conformations can be found in the alkyl chains. When the barrier compresses the film further, a second phase transition, π_C, can be observed. This is from the liquid to the liquid-condensed (LC)

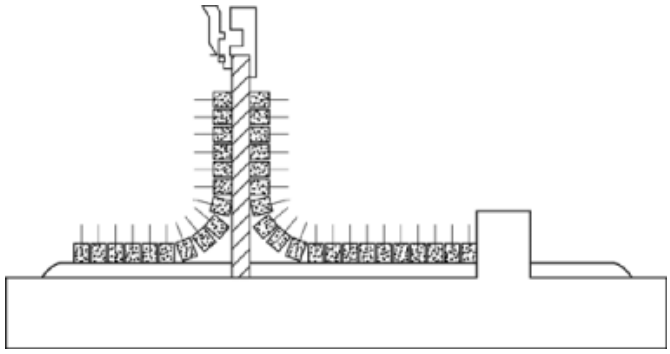

Fig. 3. Deposition of a monolayer from the water–air interface to a vertical plate.

state, where the molecules essentially are in a liquid crystalline state, and thus have some orientational order (12). The system may also undergo phase transitions between different liquid crystalline phases. The plateaus in the isotherm, where pressure does not change and area per molecule decreases, indicates an increasing orientational order.

The last phase transition is to the solid state, where molecules have both positional and orientational order. If further pressure is applied on the monolayer, it collapses, owing to mechanical instability and a sharp decrease in the pressure is observed. This collapse-pressure depends on the temperature, the pH of the subphase, and the speed with which the barrier is moved.

It was established in 1945 that monolayers of saturated fatty acids have quite complicated phase diagrams (13). However, the observation of the different phases has become possible only much more recently owing to improvements in experimental optical techniques such as fluorescence, polarized fluorescence, and Brewster angle microscopies, and x-ray methods using synchrotron radiation, etc. Thus, it has become well accepted that lipid monolayer structures are not merely solid, liquid expanded, liquid condensed, etc, but that a fairly large number of phases and mesophases exist, as a variety of phase transitions between them (14, 15).

1.2. The Transfer of Monolayers to a Solid Substrate

Two methods of transfer of monolayers from the water–air interface onto a solid substrate are important. The first, and more conventional, method is the vertical deposition (16). A monolayer of amphiphiles at the water–air interface can be deposited by the displacement of a vertical plate (Fig. 3). When such a plate is moved through the monolayer at the water–air interface, the monolayer can be transferred during immersion (retraction or upstroke) or immersion (dipping or downstroke). A monolayer is usually transferred during retraction when the substrate surface is hydrophilic, and the hydrophilic head groups interact with the surface. On the other hand, if the substrate surface is hydrophobic, the monolayer is transferred in the immersion, and the hydrophobic alkyl chains interact with the surface. If the deposition process starts with a hydrophilic substrate, the surface becomes hydrophobic after the first monolayer transfer. Thus the second monolayer is transferred in the immersion. This is the most usual mode of multilayer formation for amphiphilic molecules in which the head group is very hydrophilic and the tail is an alkyl chain. This mode is called the Y-type deposition (Fig. 4**a**). For very hydrophilic head groups, eg, –COOH, $–PO_3H_2$, etc, this is the most stable deposition mode, because the interactions between adjacent monolayers are then either hydrophobic–hydrophobic, or hydrophilic–hydrophilic. This mode produces centrosymmetric films comprised of bilayers.

Films may be formed only in downstroke (X-type, Fig. 4**b**). The deposition speed may affect the deposition mode (16, 17). If deposition occurs only when films are formed in upstroke Z-type films result (Fig. 4**c**). These are cases where the head group is not as hydrophilic, eg, $COOCH_3$ (18), or where the alkyl chain is

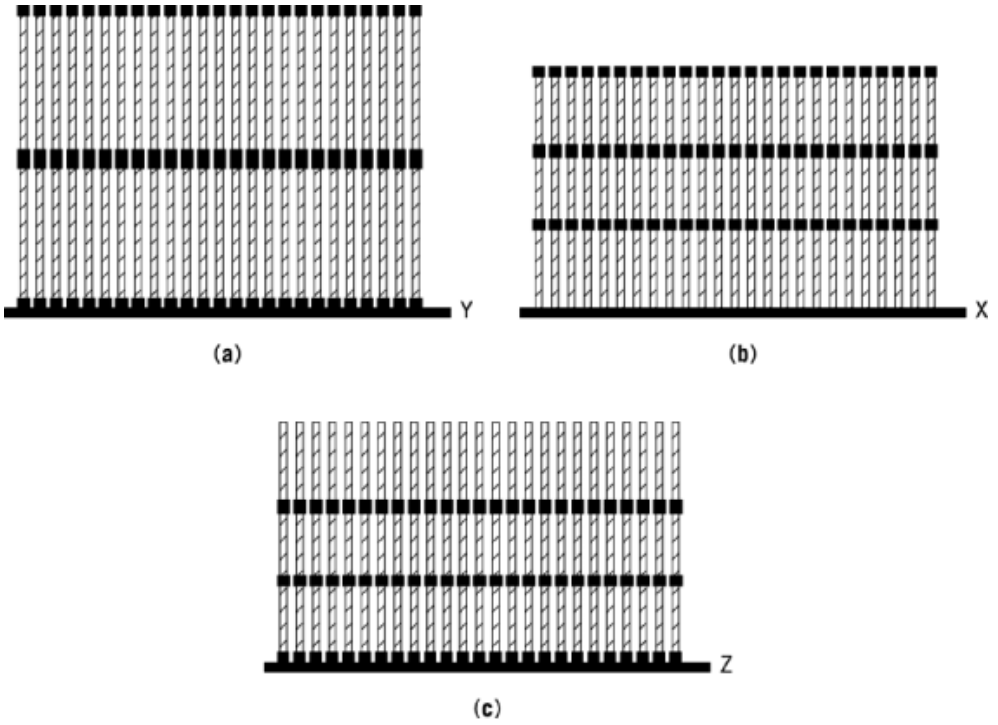

Fig. 4. Multilayer films where (□) represent a hydrophobic group and (■) a hydrophilic one: (**a**) Y-type, (**b**) X-type, and (**c**) Z-type.

terminated by a weak polar group, eg, NO_2 (19). In both cases the interactions between adjacent monolayers are hydrophilic–hydrophobic. These multilayers are therefore less stable than the Y-type systems. Both X- and Z-type depositions are noncentrosymmetric.

The amount of amphiphile that can be deposited on a glass slide depends on several factors (2). The deposition ratio is defined as A_I/A_S, where A_I is the area of the substrate coated with a monolayer, and A_I is the decrease of area occupied by that monolayer at the water–air interface, at constant pressure. An ideal Y-type film is a multilayer system having a constant transfer ratio of one for both upstroke and downstroke. An ideal X-type film can be defined accordingly as a layer system where the transfer ratio is always one for the downstroke and zero for the upstroke. In practice, there are deviations from the ideal, ie, the transfer ratio is ≤ 1, or not equal for upstroke and downstroke depositions in the case of Y-type films, or not zero in upstroke depositions for X-type films, giving a mixed X–Y-type film. This is a clear manifestation of the inherent instability of X films, because it suggests that the molecules in the X film flip over. For such X–Y films, a deposition can be defined by the ratio θ,

$$\theta = \frac{A_1^{\mathrm{u}}}{A_1^{\mathrm{d}}}$$

where $A^{\mathrm{u}}{}_1$ is the transfer ratio for the upstroke deposition, and $A^{\mathrm{d}}{}_1$ for the downstroke deposition. For an ideal Y film, $\theta = 1$; for X film, $\theta = 0$, and for Z film, $\theta = \infty$. Once the decrease of area of the monolayer at the water–air interface is plotted as a function of time during the deposition process, the deposition ratio for successive layers can be measured, and information on the deposition nature obtained.

Another way of building LB multilayer structures is the horizontal lifting or Schaefer's method introduced in 1938 (20). Schaefer's method is useful for the deposition of very rigid films, which are at the two-dimensional-solid region in the π-A diagram (Fig. 3). In this method, a compressed monolayer is formed at the water–air interface and then a flat substrate is placed horizontally on the monolayer film. When this substrate is lifted and separated from the water surface, the monolayer is transferred onto the substrate, in theory, keeping the same molecular direction (X-type, Fig. 4**b**). The deposition of high quality X-type LB films of ethyl stearate and octadecyl acrylate using a fully automated horizontal lifting has been reported (21, 22). However, cadmium and lanthanum arachidate give LB films having x-ray diffraction corresponding to Y-type deposition, thus indicating that those molecules turn over either during, or after deposition. Monolayers of polymeric amphiphiles may be good candidates for horizontal lifting because of their high viscosity.

1.3. LB Films of Long-Chain Fatty Acids

LB films of saturated long-chain fatty acids have been studied since the inception of the LB technique. The most stable films of long-chain fatty acids are formed by cadmium arachidate deposited from a buffered $CdCl_2$ subphase. These films, considered to be standards, have been widely used as spacer layers (23) and for examining new analytical techniques. Whereas the chains are tilted $\sim 25^\circ$ from the surface normal in the arachidic acid, $CH_3(CH_2)_{18}COOH$, films (24), it is nearly perpendicular to the surface in the cadmium arachidate films (25).

LB films of ω-tricosenoic acid, $CH_2{=}CH{-}(CH_2)_{20}COOH$, have been studied as electron photoresists (26–28). A resolution better than 50 nm could be achieved. Diacetylenic fatty acids have been polymerized to yield the corresponding poly(diacetylene) derivatives that have interesting third-order nonlinear optical properties (29).

1.4. LB Films of Liquid-Crystalline Amphiphiles

Liquid-crystal (LC) phases are materials that have inherently ordered-layer structures, formed by self-organization of mesogenic compounds (30) (see Liquid crystalline materials). Therefore, by having a liquid-crystalline group in an amphiphile, enhanced order, thermal stability, and interesting physical properties can result. Furthermore, the study of liquid crystals at the water–air interface in a systematic way should add to the understanding of the two-dimensional organization, and the effect of the director on the relative orientation of molecules in the layers of a multilayer film. There have been a large number of studies on LB films of LCs (4).

Investigations of a terphenyl LC compound **(1)** showed that the hydrophilicity of the substrate and the ratio of the LC and CA determined the mode of transfer (31). The material has a short (C_5) alkyl chain and a weak hydrophilic headgroup (CN). The pure LC gives Z-type deposition on hydrophilic substrates. The head group is not highly hydrophilic. On the other hand, on hydrophobic surfaces, the deposition starts as Y-type, but gradually changes to Z-type. The inherent order of the LC material may be high enough so that a very short alkyl chain can be used. Furthermore, the order is given by the LC unit and there is no need for a strong hydrophilic head group. Therefore, Z-type deposition becomes more stable, and even preferred.

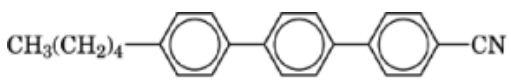

(1)

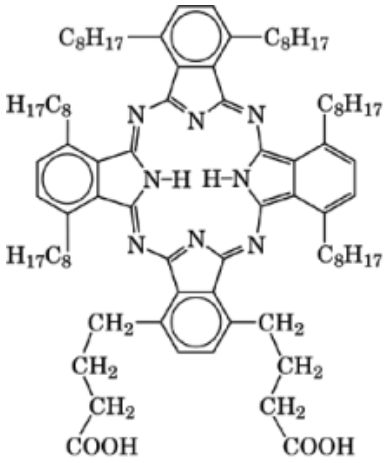

(2)

LB films of 1,4,8,11,15,18-hexaoctyl-22,25-bis-(carboxypropyl)-phthalocyanine **(2)**, an asymmetrically substituted phthalocyanine, were stable monolayers formed at the water–air interface that could be transferred onto hydrophilic silica substrates (32–34). When a monolayer film of the phthalocyanine derivative was heated, there was a remarkable change in the optical spectrum. This, by comparison to the spectrum of the bulk material, indicated a phase transition from the low temperature herringbone packing, to a high temperature hexagonal packing.

1.5. LB Films of Porphyrins and Phthalocyanines

The porphyrin is one of the most important among biomolecules. The most stable synthetic porphyrin is 5,10,15,20-tetraphenylporphyrin (TPP). Many porphyrin and phthalocyanine (PC) derivatives form good LB films. Both these molecules are important for applications such as hole-burning that may allow information storage using multiple frequency devices. In 1937 multilayers were built from chlorophyll (35).

The first synthesis of amphiphilic porphyrin molecules involved replacement of the phenyl rings in TPP with pyridine rings, quaternized with $C_{20}H_{41}Br$ to produce tetra(3-eicosylpyridinium)porphyrin bromide **(3)** (36). The pyridinium nitrogen is highly hydrophilic: the long C_{20} hydrocarbon serves as the hydrophobic part. Tetra[4-oxy(2-docosanoic acid)]phenyl-porphyrin **(4)** has also been used for films (37).

Tetrakis(cumylphenoxy)phthalocyanine **(5)** a PC derivative, having liquid–crystalline-like substituents (38–43) was studied because the cross-section area of the substituents is much larger than that of a normal alkyl chain, and therefore, the requirement of minimized free volume in the assembly may be easier to accomplish.

An LB film from a new amphiphilic, a two-ring phthalocyanine, (HO)GePc–O–SiPc(OSi(n-C_6H_{13})$_3$ **(6)** (44), gave monolayers at the water–air interface where the rings were parallel to the water surface. The hydrophilic OH head and the hydrophobic $Si(C_6H_{13})_3$ tail help to ensure the desired molecular orientation, as well as provide high solubility. The monolayers thus formed are stable and robust, and can be deposited to form good multilayer films. The main interest in these monolayers is their apparent high anisotropy.

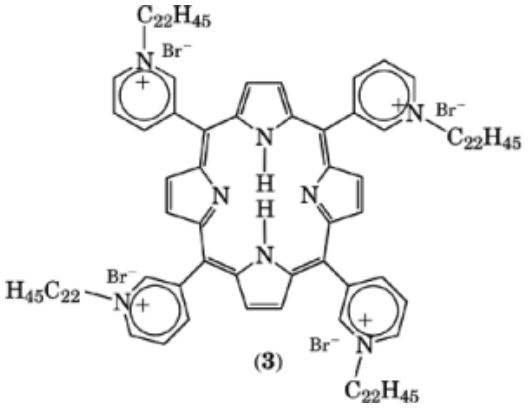

(3)

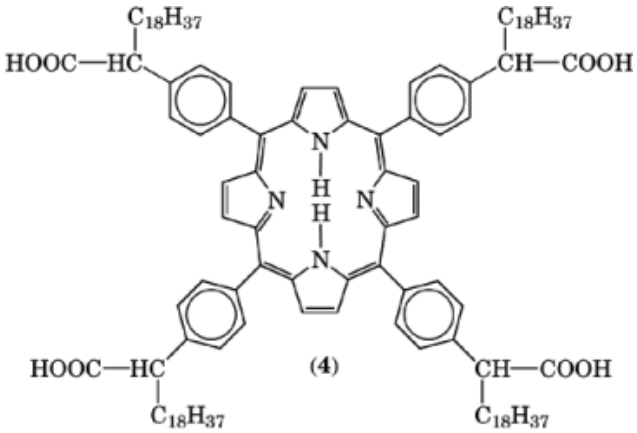

(4)

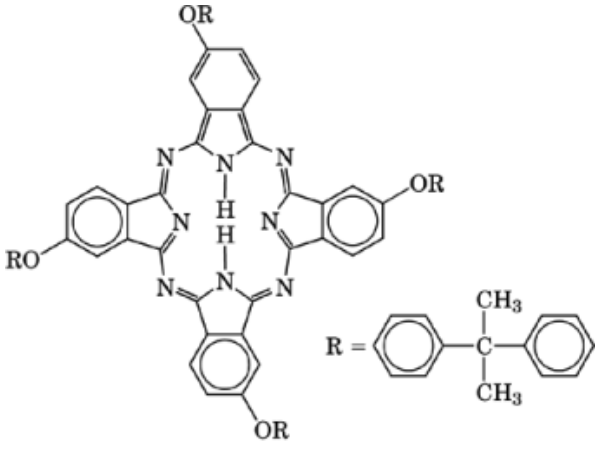

(5)

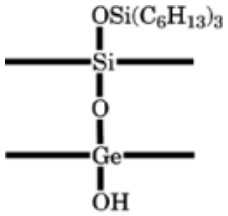

(6)

1.6. LB Films of Polymerizable Amphiphiles

Studies of LB films of polymerizable amphiphiles include simple olefinic amphiphiles, conjugated double bonds, dienes, and diacetylenes (4). In general, a monomeric amphiphile can be spread and polymerization can be induced either at the air–water interface or after transfer to a solid substrate. The former polymerization results in a rigid layer that is difficult to transfer.

In the first attempt to prepare a two-dimensional crystalline polymer (45), ^{60}Co γ-radiation was used to initiate polymerization in monolayers of vinyl stearate **(7)**. Polymerization at the air–water interface was possible but gave a rigid film. The monomeric monolayer was deposited to give X-type layers that could be polymerized *in situ*.This polymerization reaction, quenched by oxygen, proceeds via a free-radical mechanism.

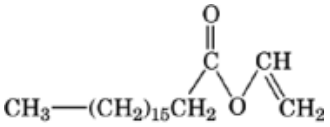

(7)

The pursuit of further miniaturization of electronic circuits has made submicrometer resolution lithography a crucial element in future computer engineering. LB films have long been considered potential candidates for resist applications, because conventional spin-coated photoresist materials have large pinhole densities and variations of thickness. In contrast, LB films are two-dimensional, layered, crystalline solids that provide high control of film thickness and are impermeable to plasma down to a thickness of 40 nm (46). The electron beam polymerization of ω-tricosenoic acid monolayers has been mentioned. Another monomeric amphiphile used in an attempt to develop electron-beam-resist materials is α-octadecylacrylic acid **(8)**.

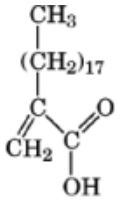

(8)

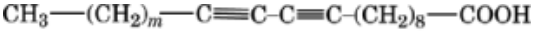

(9)

Diacetylenic amphiphiles have been studied in great detail because of the potential application of poly(diacetylene) films in nonlinear optical waveguide devices (47–51) (see Nonlinear optical materials). The early systematic studies on diacetylenic amphiphiles (52–56) showed that ultrathin polyacetylenic films of **(9)** where $m \geq 8$, are very stable and have interesting physical properties, eg, photoconductivity (57). Diacetylene polymerization requires specific arrangement of the triple bonds, because the reaction proceeds via a 1,4-addition to the conjugate triple bond (58, 59). In general, diacetylenic amphiphiles for rigid films aggregate even at zero surface pressure. Thus, they form domains at the air–water interface which make them rather useless in integrated optics application. A horizontal electric field of 104 V/m above the water surface can increase the domain size from 1–300 μm to 1 mm (60).

1.7. LB Films of Polymeric Amphiphile

Since the first successful deposition of a polymeric LB film (61), there have been a large number of studies examining different structural parameters on the transferability and stability of the polymeric LB films (4). One interesting idea for polymers for LB films is the use of a spacer group (mostly hydrophilic) to decouple the motion of the polymer from that of the lipid membrane (62, 63). Monolayers from a polymer **(10)** having hydrophilic phosphate groups and a tetraethylene oxide spacer were used to link a glycerol diether to the polymer chain (63).

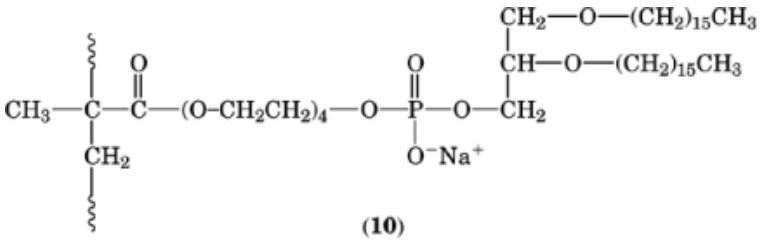

(10)

Hydrophilic spacer groups may be introduced into a polymer through the side chain, the main chain, or both. Films can be prepared using different values of monomer feed (62).

1.8. Potential Applications of LB Films

LB films have long been expected to provide new technologies and novel materials, designed at the molecular level. Commercialization of any device would, however, require much faster deposition rates than those available as of this writing (ca 1997) when there is very little activity in U.S. Industrial laboratories.

Serious attempts to use LB films in commercial applications include the use of lead stearate as a diffraction grating for soft x-rays (64). Detailed discussion on applications of LB films are available (4, 65). From the materials point of view, the ability to build noncentrosymmetric films having a precise control on film thickness, suggests that one of the first applications of LB films may be in the area of second-order nonlinear optics. Whereas a waveguide based on LB films of fatty acid salts was reported in 1977, a waveguide based on polymeric LB films has not yet been commercialized.

In 1983 the first paper on SHG from LB multilayers (66), using 4-octadecylamino-4′-nitroazobenzene **(11)** as the amphiphile, was reported.

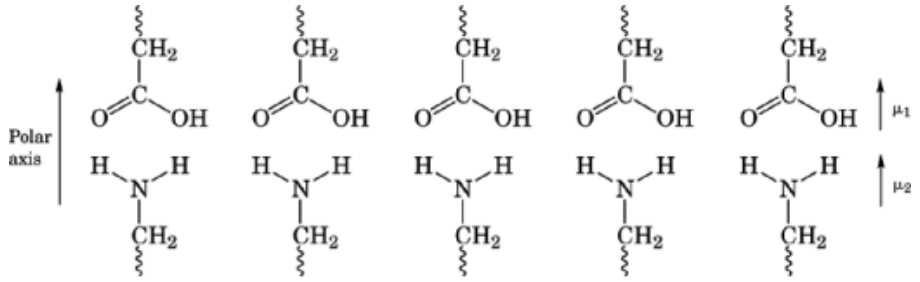

Fig. 5. Interaction between fatty acids and amines to produce an ABAB film having a polar axis.

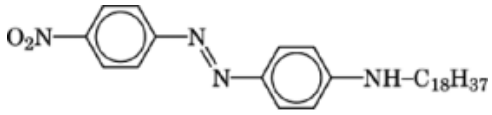

(11)

A monolayer of the pyridine-substituted alkyl merocyanine **(12)** was prepared in the 1970s (67), and a noncentrosymmetric multilayer structure of merocyanine amphiphiles was later prepared (68) using derivatives, but introducing long-chain amines as the counter layer in an ABABAB system (69, 70).

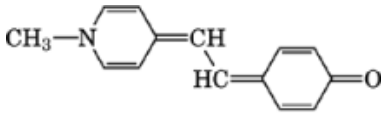

(12)

In the mid-1980s, SHG was measured from a merocyanine LB film (71) giving a value of 2.42×10^{-27} cm^5/esu for β_z of the dye. This is a very high number and may be resonance-enhanced at 2ω (533 nm).

An amphiphile having amide groups **(13)** in the alkyl chain, thus introducing H-bonding in addition to the van der Waals interaction, was prepared (20). A *p*-nitroaniline chromophore was used at the end of the alkyl group, allowing for hydrogen bonding to stabilize a Z-type multilayer.

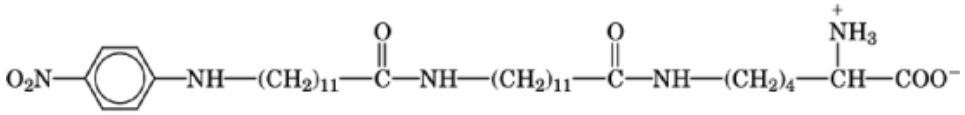

(13)

Alternate-layer LB films (Y-type, ABAB) of long-chain amines and fatty acids may be used for pyrroelectric applications (Fig. 5). Stearylamine, $C_{18}H_{37}NH_2$, and a series of straight-chain fatty acids, yield a thick film (several hundreds of monolayers) which gave a pyrroelectric coefficient of ~0.05 $nC/(cm^2 \cdot K)$ (72). A coefficient of 0.3 $nC/(cm^2 \cdot K)$ for an 11-monolayer sample of ω-tricosenoic acid and docosylamine $C_{22}H_{45}NH_2$ has been reported (73).

In pyrroelectric devices, a charge is developed across the film in response to heating and such devices may serve as ir-detectors (see Infrared technology and raman spectroscopy). Piezoelectric applications are promising as sound detectors, because for these, a charge is developed across the film in response to pressure. A review is available (74).

The area of photoinduced electron transfer in LB films has been established (75). The ability to place electron donor and electron acceptor moieties in precise distances allowed the detailed studies of electron-transfer mechanism and provided experimental support for theories (76). This research has been driven by the goal of understanding the elemental processes of photosynthesis. Electron transfer is, however, an elementary process in applications such as photoconductivity (77–79), molecular rectification (79–84), etc.

Chemical and biological sensors (qv) are important applications of LB films. In field-effect devices, the tunneling current is a function of the dielectric constant of the organic film (85–90). For example, NO_2, an electron acceptor, has been detected by a phthalocyanine (or a porphyrin) LB film. The mechanism of the reaction is a partial oxidation that introduces charge carriers into the film, thus changing its band gap and as a result, its dc-conductivity. Field-effect devices are very sensitive, but not selective.

One of the most promising optical devices is that of the surface plasmon resonance (spr) (91). Surface plasmons are collective oscillations of the free electrons at the boundary of a metal and a dielectric. The surface plasmons are guided waves (92), and their resonance conditions are very sensitive to changes in the thickness and refractive index of the medium adjacent to the metal. Spr has been used to investigate the interaction between NO_x and LB films of tetra-4-*tert*-butylphthalocyanine-containing silicon (93). Another optical detector of toxic gases was demonstrated using fluorescent porphyrin LB films (94). Changes in fluorescence for NO_2, HCl, and Cl_2 gases were reported. The fluorescence could be quenched quantitatively in the cases of both NO_2 and HCl using NH_3 vapor. Oxygen could be detected using phosphorescent LB films of tetraphenylporphyrin palladium (95). A surface acoustic wave (SAW) oscillator incorporating LB films had a detection limit of 40 ppb NO_2 in dry air (84). The subject of chemical sensors has been reviewed (96).

The search for microbiosensors has brought the need for highly selective and highly sensitive organic layers, with tailored biological properties that can be incorporated into electronic, optical, or electrochemical devices (97). From the materials point of view, LB films are an excellent choice because of the high control on their chemical structure at the molecular level, and the ability to incorporate into them large biomolecules molecules. The limitation, however, is that these can be transferred only onto a flat surface and cannot, for example, be coated on an optical fiber. Also, it is difficult to imagine the transfer of an LB film onto a substrate having a very small surface area. Examples of biosensors using LB films appear in References (98–105) (see Biosensors).

2. Self-Assembled Monolayers

The formation of monolayers by self-assembly of surfactant molecules at surfaces is one example of this general phenomenon. In nature, self-assembly results in supermolecular hierarchical organizations of interlocking components providing very complex systems (106). In 1946 as account was published of the preparation of monomolecular layers by adsorption (self-assembly) of a surfactant onto a clean metal surface (107). In the 1980s it was shown that self-assembled monolayers (SAMs) of alkanethiolates on gold can be prepared by adsorption of di-*n*-alkyl disulfides from dilute solutions (108). Many self-assembly systems have since been investigated, but monolayers of alkanethiolates on gold are probably the most studied.

The ability to tailor both head and tail groups of the constituent molecules makes SAMs excellent systems for a more fundamental understanding of phenomena affected by competing intermolecular, molecular–substrate and molecule–solvent interactions, such as ordering and growth, wetting, adhesion, lubrication, and corrosion. Because SAMs are well-defined and accessible, they are good model systems for studies of physical chemistry and statistical physics in two dimensions, and the crossover to three dimensions.

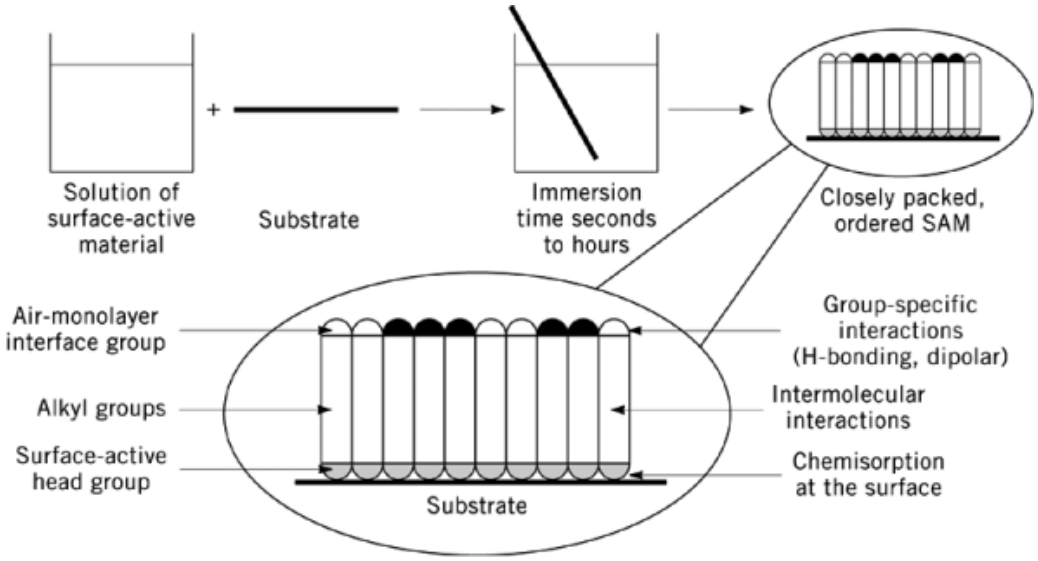

Fig. 6. Self-assembled monolayers are formed by immersing a substrate into a solution of the surface-active material. Necessary conditions for the spontaneous formation of the 2-D assembly include chemical bond formation of molecules with the surface, and intermolecular interactions.

SAMs provide the needed design flexibility, both at the individual molecular and at the material levels, and offer a vehicle for investigation of specific interactions at interfaces, and of the effect of increasing molecular complexity on the structure and stability of two-dimensional assemblies. These studies may eventually produce the design capabilities needed for assemblies of three-dimensional structures (109).

The interest in the general area of self-assembly, and specifically in SAMs, stems partially from the perceived relevance to science and technology. In contrast to ultrathin films made by, for example, molecular beam epitaxy (MBE) and chemical vapor deposition (CVD), SAMs are highly ordered and oriented and can incorporate a wide range of groups both in the alkyl chain and at the chain termina. Therefore, a variety of surfaces having specific interactions can be produced with fine structural control (110). Owing to their dense and stable structure, SAMs have potential applications in corrosion prevention, wear protection, and other areas. In addition, the biomimetic and biocompatible nature of SAMs makes their applications in chemical and biochemical sensing promising. Their high molecular order parameter in SAMs makes them ideal as components in electrooptic devices. Work on nanopatterning of SAMs suggests that these systems may have applications in patterning of GaAs, and in the preparation of sensor arrays (111).

SAMs are ordered molecular assemblies formed by the adsorption (qv) of an active surfactant on a solid surface (Fig. 6). This simple process makes SAMs inherently manufacturable and thus technologically attractive for building superlattices and for surface engineering. The order in these two-dimensional systems is produced by a spontaneous chemical synthesis at the interface, as the system approaches equilibrium. Although the area is not limited to long-chain molecules (112), SAMs of functionalized long-chain hydrocarbons are most frequently used as building blocks of supermolecular structures.

Herein the focus is on SAMs of trichlorosilanes and thiols. SAMs of carboxylic acids are important as a connection between the LB and self-assembly techniques, but studies of their formation and structure have been relatively limited. SAMs of carboxylic acids on Al_2O_3, AgO, and CuO have also been carried out (113–124).

2.1. Monolayers of Organosilicon Derivatives

SAMs of alkylchlorosilanes, alkylalkoxysilanes, and alkylaminosilanes require hydroxylated surfaces as substrates for their formation. The driving force for this self-assembly is the *in situ* formation of polysiloxane, which is connected to surface silanol groups (–Si–OH) via Si–O–Si bonds. Substrates on which these monolayers have been successfully prepared include silicon oxide (125–130), aluminum oxide (131, 132), quartz (133–135), glass (130), mica (136–138), zinc selenide (131, 132), germanium oxide (130), and gold (139–141). OTS monolayers on silicon oxide and on gold activated by uv-ozone exposure have been compared by ir spectroscopy, ellipsometry, and wetting measurements showing identical average film structures (142).

High quality SAMs of alkyltrichlorosilane derivatives are not simple to produce, mainly because of the need to carefully control the amount of water in solution (126, 143, 144). Whereas incomplete monolayers are formed in the absence of water (127, 128), excess water results in facile polymerization in solution and polysiloxane deposition of the surface (133). Extraction of surface moisture, followed by OTS hydrolysis and subsequent surface adsorption, may be the mechanism of SAM formation (145). A moisture quantity of 0.15 mg/100 mL solvent has been suggested as the optimum condition for the formation of closely packed monolayers. X-ray photoelectron spectroscopy (xps) studies confirm the complete surface reaction of the $–SiCl_3$ groups, upon the formation of a complete SAM (146). Infrared spectroscopy has been used to provide direct evidence for the full hydrolysis of methylchlorosilanes to methylsilanoles at the solid/gas interface, by surface water on a hydrated silica (147).

Temperature has been found to play an important role in monolayer formation. The threshold temperature below which an ordered monolayer is formed is a function of the chain length, being higher (18°C) for an octadecyl than for a tetradecyl chain (10°C) (126). The issue is the competition between the reaction of hydrolyzed (or partially hydrolyzed) trichlorosilyl groups and other such groups in solution to form a polymer, and the reaction of such groups with surface Si–OH moieties to form a SAM. As temperature decreases, the preference for surface reaction increases. Moreover, as temperature decreases, reaction kinetics decrease as well, resulting in the diminution of thermal disorder in the forming monolayer, the formation of an ordered assembly, and the gain of van der Waals (VDW) energy. Solid-state ^{13}C nmr studies of OTS monolayers deposited on fumed silica particles have confirmed these results (148).

Substrates used in the formation of silane SAMs are amorphous; thus the packing and ordering of alkyl chains in SAMs of alkyl silanes are determined by the underlying structure of the surface polysiloxane chain. A schematic description of a polysiloxane at the monolayer substrate interface is shown in Figure 7. In this trimer, siloxane oxygen atoms occupy the equatorial positions and the alkyl chains are connected to the axial positions. The interchain distance is ca 0.44 nm, leaving very little free volume. This should require very little or no chain tilt. The connection between free volume and tilt is a general one, because the driving force for tilt is the reestablishment of van der Waals (VDW) contact among chains.

Alkyl chains in OTS monolayers of SiO_2 and oxidized gold are tilted at $10 \pm 2^\circ$ from the normal and there is a significant gauche defect content at the chain termina (142). Based on both ellipsometry, and the concentration of gauche defects, it was concluded that the monolayer is $\sim 96 \pm 4\%$ of the theoretical maximum coverage, which explains the observed average tilt. An important conclusion of this study is that surface hydration is responsible for decoupling of film formation from surface chemistry and the observed high film quality. Increasing the surface attachment of the forming siloxane chain through surface Si–OH groups introduces disorder and film defects.

Near edge x-ray absorption fine structure spectroscopy (nexafs) and x-ray photoelectron spectroscopy (xps) have been used to study SAMs of OTS, octadecyltrimethoxysilane (OTMS), $CH_3(CH_2)_{17}Si(OCH_3)_3$, and (17-aminoheptadecyl)-trimethoxysilane (AHTMS), $H_2N(CH_2)_{17}Si(OCH_3)_3$ (149). A number of important observations have been reported. First, the chains in OTS SAMs are practically perpendicular to the substrate surface (tilt angle $0 \pm 5^\circ$). Second, the adsorption mechanisms of trichlorosilane and trimethoxysilane groups are different, resulting in a higher ($20 \pm 5^\circ$) tilt angle of the chains in OTMS SAMs. Third, the introduction

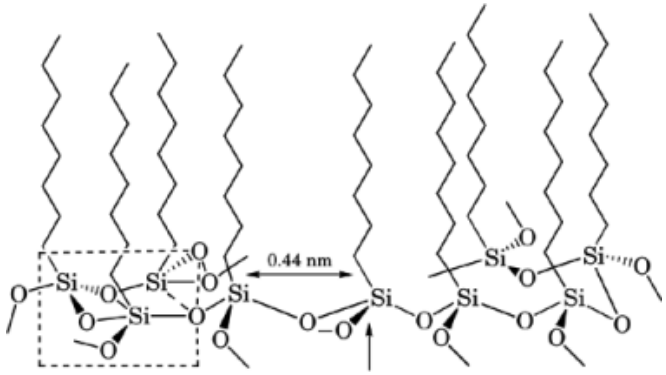

Fig. 7. Schematic description of a polysiloxane at the monolayer–substrate surface (4). The arrow points to an equatorial Si–O bond that can be connected either to another polysiloxane chain or to the surface. The dashed line on the left is a bond in a possible precursor trimer where the alkyl chains can occupy either axial or equatorial positions.

of a polar amino group at the chain termina results in a more disordered monolayer, probably as a result of acid–base interactions with surface silanol groups. This last observation suggests that when such interactions exist, a preferred route may be to create surface functionalities by chemical reactions.

The reproducibility of alkyltrichlorosilane monolayers remains a problem. The quality of the monolayer formed is very sensitive to reaction conditions (126, 127, 150). Hexadecane may or may not be incorporated in OTS monolayers (129, 143). It has been suggested that partial OTS monolayers have heterogeneous island structure (129, 151). These incomplete monolayers may, however, be homogeneous and disordered (r134,r135,r146,r152,r153). More recently atomic force microscopy (afm) studies have confirmed the island structure of partial monolayers. The adsorption of OTS onto glass and silicon oxide surfaces (150) and on mica (138) results in monolayers on mica by nucleating isolated domains, where the fractal dimensions increase with increased surface coverage. Other afm images of OTS SAMs on mica and on silica and silicon have also been produced (154–161). Pin holes in the OTS films from several nanometers to 100 nm in diameter, in monolayers on mica formed by self-assembly from a solvent mixture have been observed (154). Studies of OTS SAMs on silicon indicate that in order to obtain reproducible, good quality films, samples must be prepared under class 100 clean room conditions (158). OTS SAMs form on silicon, first by growth of large islands and then by filling-in with smaller islands until the film is complete. This growth mechanism has been utilized to form binary SAMs of OTS and 11-(2-naphthyl)undecyltrichlorosilane (162). Other researchers have suggested that in partial (25–30%) monolayers OTS molecules lie flat on the silicon surface, producing a water contact angle of 90° (159).

Differences in reported results also exist for other alkyltrichlorosilane systems. Surface coverages of vinyl-terminated alkyltrichlorosilane have been reported to be only ∼63% (163), and well-packed monolayers (126). Surface coverage for monolayers of methyl-23-trichlorosilyltricosanoate (MTST), $H_3COOC–(CH_2)_{22}–SiCl_3$, have been reported to be ∼93% (164) and full monolayers (165).

Patterns of ordered molecular islands surrounded by disordered molecules are common in Langmuir layers, where even in zero surface pressure molecules self-organize at the air–water interface. The difference between the two systems is that in SAMs of trichlorosilanes the island is comprised of polymerized surfactants, and therefore the mobility of individual molecules is restricted. This lack of mobility is probably the principal reason why SAMs of alkyltrichlorosilanes are less ordered than, for example, fatty acids on AgO, or thiols on gold. The coupling of polymerization and surface anchoring is a primary source of the reproducibility problems. Small differences in water content and in surface Si–OH group concentration may result in a significant

difference in monolayer quality. Alkyl silanes remain, however, ideal materials for surface modification and functionalization applications, eg, as adhesion promoters (166–168) and boundary lubricants (169–171).

Surface modification can be achieved either by using ω-substituted alkyl silanes, or by surface chemical reactions. SAMs have been reported from alkyltrichlorosilanes having terminal functional groups of halogen (172–176), cyanide (173), thiocyanide (173), methyl ether (172), acetate (172), thioacetate (172, 177), α-haloacetate (174), vinyl (126, 127, 163, 178–184), trimethylsilylethynyl (185), methyl ester (164, 165), and *p*-chloromethylphenyl (174, 186–189). Monolayers having low surface free energy have been prepared using partially fluorinated alkylsilanes (153, 172, 190, 191). Surface modification can also be performed using various nucleophilic substitutions on SAMs of 16-bromohexadecylsilane (173). These SAMs were converted to the 16-thiocyanatohexadecylsilane monolayers by simply treating with a 0.1 M KSCN solution in DMF for 20 h. Similarly, NaN_3, Na_2S, and Na_2S_2 gave complete conversions of the bromo-terminated monolayers, as was evident from x-ray photoelectron spectroscopy (xps) (173). Reduction of the thiocyanato, cyanide, and azide surfaces by $LiAlH_4$ gave the mercapto-, and amino-terminated monolayers in complete conversions (173). Oxidation of the ω-thiol group gave sulfonic acid surfaces (173). XPS investigations of nucleophilic substitution at chain termina of alkyltrichlorosilane monolayers, using *p*-nitrothiophenolate as the nucleophile, have been carried out (174). The reaction rates obey the following order of leaving groups $I > Br > Cl$, and $X–CH_2–CO > C_6H_5–CH_2–X > CH_2–CH_2–X$. Competition reactions using thiolates and amines as nucleophiles show a clear thiolate preference. Reactions using small peptide fragments having cysteine moieties as the nucleophiles resulted in grafting of the monolayer surface with these peptides, which may be important for the development of biosensors. Patterned SAMs formed by microcontact printing of alkyltrichlorosilane on Al_2O_3/Al, SiO_2/Si, and TiO_2/Ti open new opportunities for preparation of sensors and electrooptical devices (192, 193).

Surface modification reactions are important not only for engineering surface energy and interfacial properties such as wetting, adhesion, and friction, but also for providing active surfaces for the attachment of molecules having different properties. One example is the reaction of bromo-terminated alkylsilane monolayers with the lithium salt of 4-methylpyridine to provide pyridine surfaces (175, 176). Such surfaces react with palladium (194), rhenium (176), and osmium complexes (175), and provide immobilization of organometallic moieties. Immobilized OsO_4 reacts with C_{60}-buckyballs, resulting in the formation of a C_{60}-monolayer (175). Similar monolayers can be formed by the reaction of buckyballs with amino or azido surface groups (195–197). A cysteine-specific surface was prepared for the fabrication of metalloprotein nanostructures (198). These examples show the opportunities SAMs provide in the construction of layers and of new materials by combinations thereof.

Mixed monolayers provide an excellent route for surface engineering at the molecular level. Hence, by coadsorption of alkyltrichlorosilane with different ω-functionalities, surface free energy and chemical reactivity can be designed via the control of surface chemical functionalities. However, there are few reports on mixed monolayers of alkyltrichlorosilane, and most investigations were carried out on alkanethiolate monolayers on gold. When mixed monolayers of alkyltrichlorosilane and ω-vinyl or ω-2-naphthyl alkyltrichlorosilane were prepared by competitive adsorption, it was found that the composition of the monolayer is equal to the composition of the immersion solution (127, 128, 134). The gradual increase of the amount of excimers observed with the gradual increase of the naphthyl concentration supports the ideal mixing of the two silanes in the monolayer. When the preparation of mixed monolayers of alkyltrichlorosilanes having different chain lengths was investigated, ideal mixing was observed. The composition was determined by the relative rates of adsorption of the components (199).

Construction of multilayers requires that the monolayer surface be modified to a hydroxylated one. Such surfaces can be prepared by a chemical reaction and the conversion of a nonpolar terminal group to a hydroxyl group. Examples of such reactions are the $LiAlH_4$ reduction of a surface ester group (165), the hydroboration–oxidation of a terminal vinyl group (127, 163), and the conversion of a surface bromide using silver chemistry (200). Once a subsequent monolayer is adsorbed on the "activated" monolayer, multilayer films may be built by repetition of this process (Fig. 8).

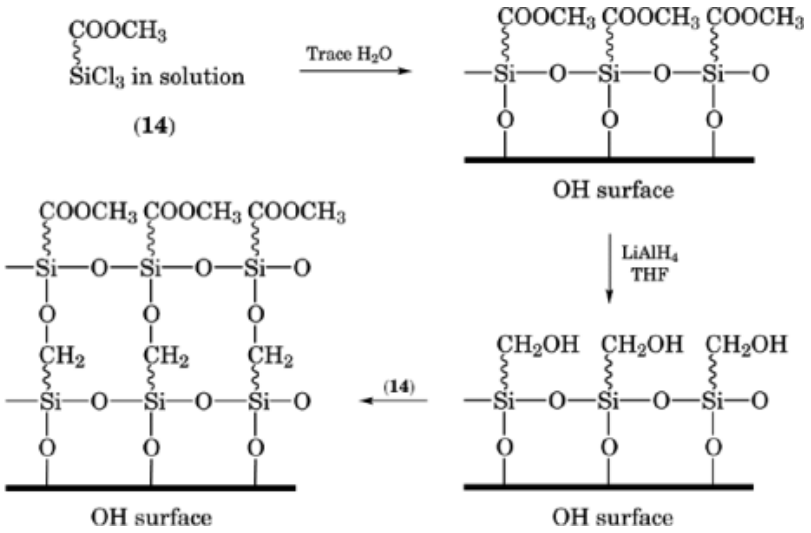

Fig. 8. Construction of self-assembled multilayers from methyl 23-trichlorosilyltricosanoate.

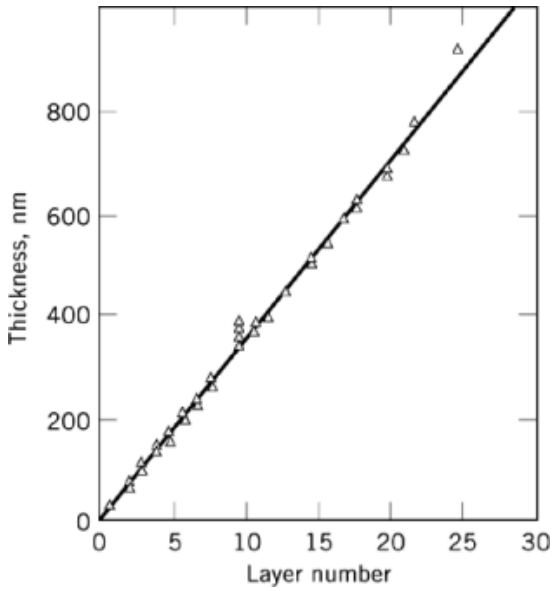

Fig. 9. Film thickness vs layer number (165).

Using this strategy, construction of multilayer films of $\sim 0.1\ \mu m$ thickness by self-assembly of methyl 23-trichlorosilyltricosanoate (MTST) on silicon substrates has been demonstrated (Fig. 9) (165). The linear relationship between the film thickness and the layer number showed a slope of 3.5 nm/layer. Ellipsometry data, absorbance intensities, and dichroic ratios for the multilayers all suggest that the samples were composed of distinct monolayers. However, ir data indicated that there may be more tilting or disordering of the alkyl chains in the seven-layer sample than for the monolayer samples.

Despite the increasing level of monolayer disorder, the preparation of a multilayer film having thickness of ∼0.1 mm was possible, indicating that the *in situ* formation of a polysiloxane backbone at the substrate–solution interface allows the monolayer to bridge over defects, such as pinholes and unreduced carbonyl groups. This repair mechanism may be very significant, because the construction of very thick films (1–2 μm, 250–500 layers) by self-assembly can be considered unlikely if defects inevitably propagate and grow.

Synchrotron x-ray diffraction studies were performed on a fifteen-layer thin film of MTST (201). The specular profile suggested a compression of the outermost layers from an average spacing of 3.190 ± 0.002 nm, which is interpreted as an increase in disordering near the film–air interface. Rocking curves of the specular profile suggest extremely rigid $–SiO_2–$ layers. In-plane results also depict rigid $–SiO_2–$ layers having spacing of 0.135 ± 0.003 nm and an increase in disorder at below critical angle measurements. The alkyl chains were shown to be hexagonally packed between these rigid layers. There was no observance of a chain tilt. A self-assembly strategy, where a $–SiCl_3$ group is attached to a small molecule, and an S_N2 reaction of the SAM introduced to a monolayer of nonlinear optically (NLO) active dyes has been developed. These were used in the construction of SAMs having second-harmonic nonlinear optical (NLO) properties (185–189). A significant improvement in the synthesis of multilayer structure reported recently is summarized in Figure 10. Using the process described in Figure 10, a three-layer system was prepared in one hour (202).

Hydrogen-bonded multilayers of self-assembling silanes have been reported (203, 204). Using a combination of ftir spectroscopy and x-ray scattering a multilayer structure was observed as having district monolayers, coupled to each other in a flexible, nonepitaxial manner, via interlayer multiple hydrogen bonds. The hydrocarbon chains are perpendicular to the layer plane: a lateral packing density is 2.1 nm/molecule; and a positional coherence length is of ca 7.0 nm.

19-Trimethylsilyl-18-nonadecynylsilane monolayers can be polymerized to the corresponding polyacetylene systems (185). The treatment of the nonpolymerized monolayers with electron-beam radiation is dependent on ambient conditions. When irradiation was carried out under helium, the result was cross-linked monolayers; however, irradiation under nitrogen yielded cross-linking accompanied by the formation of amino terminal groups; and when irradiation was carried out under oxygen, cross-linked monolayers having hydroxyl, aldehyde, and carboxylic acid terminal groups were obtained. Using this technique, it was possible to fabricate well-ordered multilayer films (184) but, having a nonlinear relationship between film thickness and the number of layers (205). Attempts to prepare thicker films failed owing to increased disorder. A competition between irradiation damage and the formation of a new layer (205) appears to exist.

Trichlorosilane derivatives of large dye molecules are difficult to purify and owing to moisture sensitivity are hard to handle. Their organic solutions tend to become turbid rather quickly owing to the formation of insoluble polymers. Thus, solutions must be replaced frequently. An exception may be the combination of self-assembly and surface chemical reaction (186, 187, 189, 202). On the other hand, ω-substituted alkyltrichlorosilane derivatives are easy to synthesize the purify. These could be used for the engineering of surface free energy through the control of chemical functionalities in their SAMs, or as active layers for attachment of biomolecules in biosensors.

2.2. Organosulfur Adsorbates on Metal and Semiconductor Surfaces

Sulfur compounds (qv) and selenium compounds (qv) have a strong affinity for transition metal surfaces (206–211). The number of reported surface-active organosulfur compounds that form monolayers on gold includes di-*n*-alkyl sulfide (212, 213), di-*n*-alkyl disulfides (108), thiophenols (214, 215), mercaptopyridines (216), mercaptoanilines (217), thiophenes (217), cysteines (218, 219), xanthates (220), thiocarbaminates (220), thiocarbamates (221), thioureas (222), mercaptoimidazoles (223–225), and alkaneselenoles (226) (Fig. 11). However, the most studied, and probably most understood, SAM is that of alkanethiolates on Au(111) surfaces.

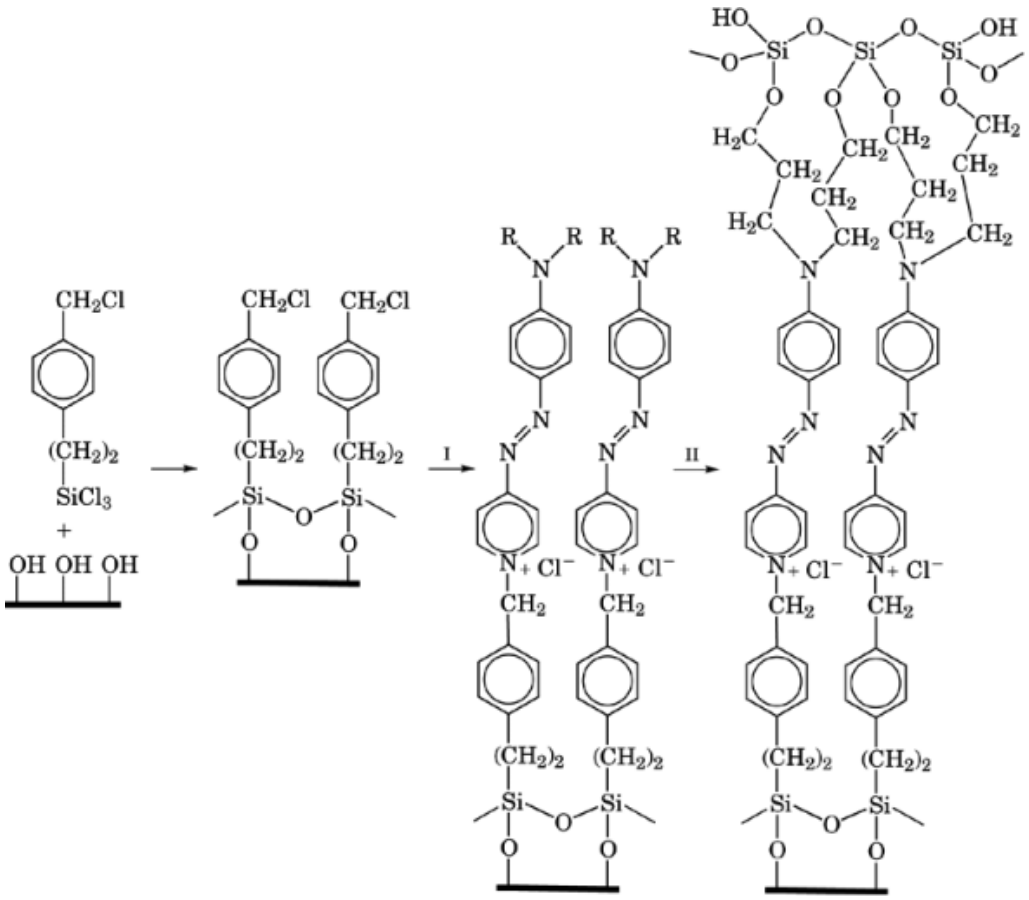

Fig. 10. Formation of noncentrosymmetric multilayer film by combining self-assembly and a surface S_N2 reaction, where R= $(CH_2)_3OH$; procedure I=spin−coating followed by annealing at 110°C; and procedure II=reaction of $Cl_3SiOSiCl_2OSiCl_3$, ie, a dilute solution of 4-[*N*,*N*,-bis-(3-hydroxypropyl)-aminophenylazo]-4′-pyridine on a benzyl chloride SAM surface was used, resulting in facile formation of SAMs having high order parameters.

It has been suggested that gold does not have a stable surface oxide (227), and therefore, its surface can be cleaned simply by removing the physically and chemically adsorbed contaminants. However, more recently it has been shown that oxidation of gold by uv and ozone at 25°C gives a $1.7 \pm 0.4 - \text{nm}$ thick Au_2O_3 layer (228), stable to extended exposure to ultra high vacuum (UHV) and water and ethanol rinses.

Organosulfur compounds coordinate very strongly also to silver (229–233), copper (231–234), platinum (235), mercury (236, 237), iron (238, 239), nanosize γ-Fe_2O_3 particles (240), colloidal gold particles (241), GaAs (242), and InP surfaces (243). Octadecanethiol monolayers provide an excellent protection of the metal surface against oxidation (234). For example, silver surfaces having octadecanethiolate monolayers could be kept in the ambient without tarnishing for many months; copper surfaces coated with the same monolayer sustain dilute nitric acid (244).

Kinetic studies of alkanethiol adsorption onto Au(111) surfaces have shown that at relatively dilute $(10^{-3}M)$ solutions, two distinct adsorption kinetics can be observed: a very fast step, which takes a few minutes, by the end of which the contact angles are close to their limiting values and the thickness about 80–90% of its maximum; and a slow step, which lasts several hours, at the end of which the thickness and

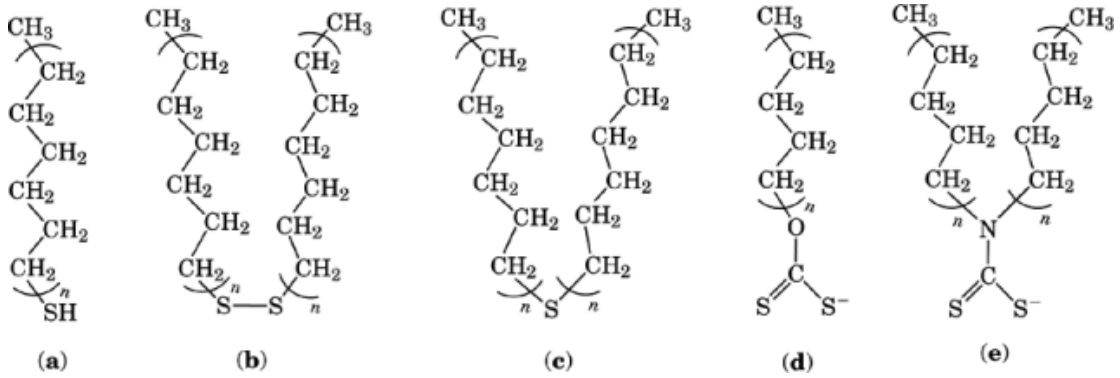

Fig. 11. Surface-active organosulfur compounds that form monolayers on gold: (**a**) alkanethiol; (**b**) dialkyl disulfide; (**c**) dialkyl sulfide; (**d**) alkyl xanthate; and (**e**) dialkylthiocarbamate.

contact angles reach their final values (245). The initial step is described well by diffusion-controlled Langmuir adsorption, and strongly depends on thiol concentration. At 1 m*M* solution the first step was over after ∼1 minute, while it required over 100 minutes at 1 mM concentration (245). The second step can be described as a surface crystallization process, where alkyl chains get out of the disordered state and into unit cells, thus forming a two-dimensional crystal. Therefore, the kinetics of the first step is governed by the surface-head-group reaction, and the activation energy may depend on the electron density of the adsorbing sulfur. On the other hand, the kinetics of the second step is related to chain disorder, eg, gauche defects; the different components of chain–chain interaction, eg, VDW, dipole–dipole, etc; and the surface mobility of chains. The kinetics are faster for longer alkyl chains, probably owing to the increased VDW interactions (245).

Second-harmonic generation, and xps measurements (246, 247), as well as near edge X-ray absorption fine structure spectroscopy (nexafs) studies confirm the two-step mechanism (248). Studies also showed pronounced differences between the short ($n < 9$) and long ($n > 9$) alkanethiolates, probably owing to the decreased rate of the second step which results from the diminution of the interchain VDW attraction energy. In the case of simple alkyl chains, the masking of adsorption sites by disordered chains is not a serious problem. However, if the chain contains a bulky group, the two steps are coupled, and the chemisorption kinetics is greatly impeded by the chain disorder (249). A direct competition between *tert*-butylmercaptan and *n*-octadecylmercaptan reveals that the latter adsorbed onto gold at greater efficiency than the former by a factor of 290–710 from ethanol (250). The additive effects of the stabilizing van der Waals interactions in the *n*-alkyl mercaptan monolayer and the sterically hindered *tert*-butylmercaptan explain the clear preference of the linear molecules.

Chemisorption of alkanethiols as well as of di-*n*-alkyl disulfides on clean gold gives indistinguishable monolayers (251) probably forming the Au(l) thiolate species. A simple oxidative addition of the S–S bond to the gold surface is possibly the mechanism in the formation of SAMs from disulfides:

$$\mathrm{R{-}S{-}S{-}R} + \mathrm{Au}_n^0 \longrightarrow \mathrm{R{-}S^-Au^+{\cdot}Au}_x^0$$

The rates of formation of SAMs from dialkyl disulfides or alkanethiols were indistinguishable, but the rate of replacement of molecules from SAMs by thiols was much faster than that by disulfides (251). Reaction of an unsymmetrical disulfide, $HO(CH_2)_{10}SS(CH_2)_{10}CF_3$, and a gold surface gave SAMs containing equal proportions of the two thiolate groups (252). Replacement experiments showed that the $S(CH_2)_{10}CF_3$ group in the mixed SAMs is replaced by $S(CH_2)_{10}CN$, on exposure to the $HS(CH_2)_{10}CN$ solution in ethanol, about 10^3 times faster than the $HS(CH_2)_{10}OH$ group. This is strong support for the disulfide bond cleavage mechanism and the subsequent formation of gold thiolate species. 4-Aminobenzenethiol has been reported to be spontaneously

oxidized to 4,4′-diaminodiphenyl disulfide in the presence of gold powder (253). This, the first observation of its kind, hints that the stability of thiolate SAMs on gold may be related to the electron density on the thiolate sulfur. However, except for the report on the dimerization of alkanethiolates of Au(111) surface to form the dialkyl disulfides (254) there has been no other direct evidence supporting such a reaction.

In the alkanethiol case, the reaction may be considered formally as an oxidative addition of the S–H bond to the gold surface, followed by a reductive elimination of the hydrogen. When a clean gold surface is used, the proton probably ends as a H_2 molecule. Monolayers can be formed from the gas phase (241, 255, 256), in the complete absence of oxygen:

$$\mathrm{R{-}\!\!-S{-}\!\!-H} + \mathrm{Au}_n^0 \longrightarrow \mathrm{R{-}\!\!-S^-Au^+{\cdot}Au}_x^0 + \frac{1}{2}\mathrm{H_2}$$

The combination of hydrogen atoms at the metal surface to yield H_2 may be an important exothermic step in the overall chemisorption energetics. That the adsorbing species is the thiolate, RS–, has been shown by xps (231, 257–259), Fourier transform infrared (ftir) spectroscopy (260), Fourier transform mass spectrometry (261), electrochemistry (262), and Raman spectroscopy (263–265). The bonding of the thiolate group to the gold surface is very strong. The homolytic bond strength is approximately 167 kJ/mol (40 kcal/mol) (206).

Based on the bond energies of RS–H, 364 kJ/mol (87 kcal/mol); H_2, 435 kJ/mol (104 kcal/mol); and RS–Au, 167 kJ/mol (40 kcal/mol), the net energy for adsorption of alkanethiolates on gold would be ca -20.9 kJ/mol (-5 kcal/mol) (exothermic). A value of -23.0 kJ/mol (-5.5 kcal/mol) has been calculated using electrochemical data (266), suggesting that the estimate of 167 kJ/mol for the S–Au bond strength is a good one. Based on similar calculations the value of ca -100 kJ/mol (-24 kcal/mol) was estimated for the adsorption energy of dialkyl disulfide, or -50 kJ/mol (-12 kcal/mol) per RS^-. This is about twice as favorable as the adsorption energy calculated for the thiol mechanism involving molecular hydrogen (266). In view of the disulfide picture (254), desorption data applied to first order kinetics, gave a better correlation than for second order kinetics (266). This, however, cannot be considered as direct evidence for thiolate dimerization. It is not clear why a dialkyl disulfide molecule remains adsorbed as such, having gauche defects at the S–C bonds to allow the hydrocarbon chains to assume hexagonal close-packing, if it can simply adsorb as two all-trans alkanethiolates.

The incomplete stability of alkanethiolate SAMs can be concluded from a number of papers. Some loss in electroactivity of ferrocenyl alkathiolate SAMs upon soaking in hexane has been reported (267), although such loss was not observed when the same SAM was immersed in ethanol (268). Exposure of other electroactive SAMs to nonaqueous electrolytes also gave clues of instability (269–271). Alkanethiolates bearing radiolabeled (^{35}S) head groups have been incorporated into SAMs on a variety of substrates (266). The question of S–C bond cleavage during adsorption to yield adsorbed sulfide, S^{2-}, and thiolate, SH^-, has been raised after S–C cleavage was reported in organosulfides, R–S–R, on adsorption to gold, producing SAMs identical to those resulting from S–H breaking in the corresponding thiol or from S–S breaking in the corresponding disulfides (272). Based on coverage measurements it was concluded that if any C–S bond cleavage occurs it is minimal (266).

Thermal stability of alkanethiolate SAMs has also been addressed. Loss of sulfur from hexadecanethiolate monolayer on gold has been reported over the range of 170–230°C (267). Temperature-programmed desorption of methanethiolate SAMs on gold yielded a desorption maximum at ca 220°C (260). Detailed mass spectroscopic studies of *tert*-butanethiolate monolayers on gold showed maximum desorption at ca 200°C (272). Using radiolabeled hexadecanethiolate monolayers, a complete loss of surface sulfur at 210°C was observed with some loss occurring at 100°C (266).

Early electron diffraction studies, both high (273, 274) and low energy (275) of monolayers of alkanethiolates on Au(111) surfaces show that the symmetry of sulfur atoms is hexagonal with an S–S spacing of 0.497 nm, and calculated area per molecule of 0.214 nm^2. Helium diffraction (276) and atomic force microscopy (afm) (277) studies confirmed that the structure formed by docosanethiol on Au(111) is commensurate with the underlying gold lattice (Fig. 12). Ultra high vacuum scanning transmission microscopy (stm) studies have added

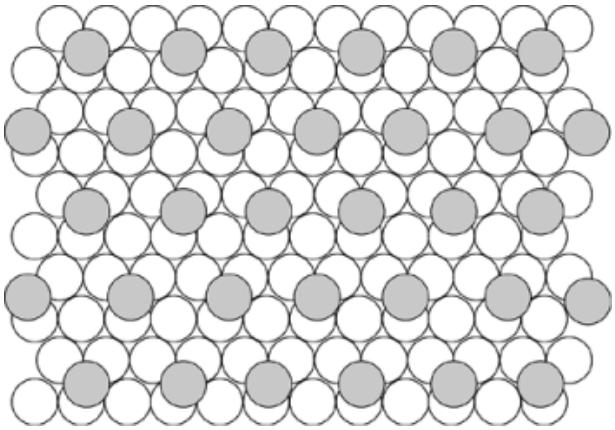

Fig. 12. Hexagonal coverage scheme for alkanethiolates on Au(111), where (○) are gold atoms and (▨) are sulfur atoms.

important information on the mechanism of SAM formation, revealing the coexistence of a two-dimensional (2D) liquid phase at room temperature of butane-, $CH_3(CH_2)_3S^-$, and hexanethiolate, $CH_3(CH_2)_5S^-$ monolayers on Au(111) (278). No 2D liquid was observed for octane-, $CH_3(CH_2)_7S^-$, and decanethiolate, $CH_3(CH_2)_9S^-$, monolayers. The short-chain homologues exhibited slow desorption of surface thiolate that led to the nucleation and growth of ordered domains. On the other hand, both octane- and decanethiolate form densely packed SAMs (279–281).

The above stm study also discovered a facile transport of surface gold atoms in the presence of the liquid phase, suggesting that the two-step mechanism does not provide a complete picture of the surface reactions, and that adsorption/desorption processes may have an important role in the formation of the final equilibrium structure of the monolayer. Support for the importance of a desorption process comes from atomic absorption studies showing the existence of gold in the alkanethiol solution. The stm studies suggest that this gold comes from terraces, where single-atomic deep pits are formed (281–283).

Ab initio calculations show that at the hollow site of Au(111), the sulfur charge is ca $-0.4e$ (211), whereas at the on-top site, this charge is ca $-0.7e$ (211). Because S–H bond cleavage occurs at the on-top site (284), if this cleavage is the rate-determining step, the adsorption rate should be faster in polar solvents, owing to the stabilization of the forming dipole. However, if the migration of a thiolate from the on-top to the hollow site is the slow step, the reaction should be faster in nonpolar solvent, owing to the diminished charge separation. Most recent second-harmonic generation studies have showed that whereas the rate constant in ethanol is 1.3×106 cm^3/(mol·sec), it is 4.7×106 cm^3/(mol·cm^3) in hexane (284), suggesting that S–H bond cleavage is not the rate-determining step.

Migration of thiolates between neighboring hollow sites is essential for healing of defects. Such migration should occur either through the on-top or the bridge sites. In both cases, the transition state is more polar than the ground state, and hence should be sensitive to dielectric constant. Indeed, ethanol has been found to yield consistently highly ordered monolayers (245). The thiolate is chemically bonded to one gold atom at the on-top site, forming a neutral gold thiolate molecule, RS–Au. This may desorb before the thiolate moves to the hollow site, thus leaving a defect. More recent stm studies suggest that some of the pinholes observed in monolayers on Au(111) may be a result of such an etching process (283). However, it is also possible that alkanethiolates desorb from the surface as $RS^-Au^+{}_3$. These pinholes disappeared after annealing the monolayers at 77 or 100°C (285, 286). If alkanethiolates increase, the mobility of gold atoms at the surface is not clear, however, the data so far indicate that surface migration of gold thiolate molecules, RS–Au, may be considered as a possible mechanism for healing monolayer defects.

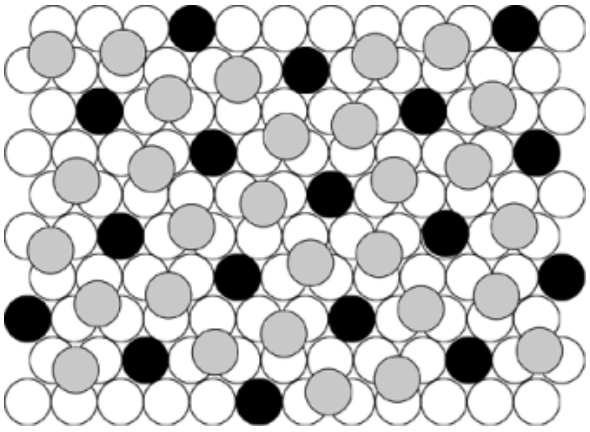

Fig. 13. A diagram showing one of the two possible $\sqrt{7}\times\sqrt{7}$ structures of alkanethiolates on Ag(111), where (○) represent the silver atoms, (•) represent thiolates at the on-top and (●) at the hollow sites.

Alkanethiolates have two binding modes at the Au(111) hollow site, one with a bend angle around the sulfur of 180° (*sp*) and the other of 104° (sp^3). The latter is being more stable by 1.7 kJ/mol (0.41 kcal/mol) (211). Thus, packing requirements may dictate the final surface–S–C angle. Many studies have suggested that this angle in monolayers on Au(111) surfaces must be tetrahedral (261). Modeling of terphenylthiolate, C_6H_5–C_6H_4–C_6H_4–S–, monolayers on Au(111) suggest a tilt angle of ∼6° from the surface normal (214), and preliminary x-ray diffraction studies of 4-methyl-4′-mercaptobiphenyl monolayers on Au(111) single-crystal surfaces confirm this suggestion (239), thus providing the first evidence that a second chemisorption mode is possible.

The energy barrier between the two chemisorption modes on Au(111) is very small, 10.5 kJ/mol, (2.5 kcal/mol), (211), suggesting that the thiolate may easily cross from one of these minima to the other, enabling a facile annealing mechanism. This predicts that changing tilt direction may occur well below the melting point of the monolayer, and should be chain-length-dependent.

X-ray data show narrowing of the diffraction peak when monolayers of alkanethiolates on Au(111) were annealed (279). A development of larger domain size was the apparent result of the heating and cooling. Thus, close packing and high ordering of alkanethiolates on Au(111) may result from the relatively easy 2-D recrystallization process, as well as from the migration of gold thiolate molecules.

Molecular mechanics (MM) energy minimization indicates that the two modes lead to monolayers exhibiting different types of packing arrangements, but comparable in their ground state energies. (The monolayer resulting from the sp^3 mode is more stable by 2.5 kJ/mol (0.6 kcal/mol)) (211). Therefore, monolayers may consist of two different chemisorption modes ordered in different domains, simultaneously coexisting homogeneous clusters, each characterized by a different conformer in their unit cell. This may explain the observation of 2D liquid in butane- and hexanethiolate monolayers on gold (278), where VDW interactions do not provide enough cohesive energy to allow for small domains to coexist as a 2D solid.

The chemisorption of S atoms (287), SH (288), and SCH_3 groups (289, 290) on Ag(111) can be described as $(\sqrt{7}\times\sqrt{7})$R10.9° (Fig. 13), having an S–S distance of 0.441 nm slightly smaller than the interchain repeat distance in crystalline paraffins of 0.465 nm (291).

For octadecanethiolate, $CH_3(CH_2)_{17}S^-$, monolayers, grazing incident x-ray diffraction (gixd) shows a lattice constant of 0.46–0.47 nm, alkyl chains that are hardly tilted, and an overlayer very similar to $(\sqrt{7}\times\sqrt{7})$R10.9°, but with 12° rotation, and an outermost Ag(111) layer slightly expanded (292). The $(\sqrt{7}\times\sqrt{7})$R10.9° requires that the thiolates at the on-top site be ca 0.05 nm higher than those residing at

the hollow site. SAMs of decanethiolate, $CH_3(CH_2)_9S^-$, on Ag(111) using ultrahigh impedance STM have been studied (293). The average nearest-neighbor distance within a domain was shown to be 0.461 ± 0.015 nm; there are two domain types corresponding to two orientations of a six-fold symmetric lattice separated by $20.7 \pm 2.3^\circ$; and fluctuations of heights of nearest neighbors far from domain boundaries are less than 0.01 nm.

Some thiophenolate monolayers also have been investigated. Thiophenolate, C_6H_5S–, forms ordered monolayers on Ag(111) with a $(\sqrt{7} \times \sqrt{3}, 88^\circ)R40.9^\circ$, and benzene rings closely packed in face-to-face stacked columns (294). Benzylthiolate (295), *p*-pyridinethiolate (296), and *o*-pyridinethiolate (296), also form ordered monolayers on Ag(111), but with fewer close-packed aromatic rings.

The ftir studies reveal that the alkyl chains in SAMs of thiolates on Au(111) usually are tilted $\sim 26 - 28^\circ$ from the surface normal, and display $\sim 52 - 55^\circ$ rotation about the molecular axis. This tilt is a result of the chains reestablishing VDW contact in an assembly with ~ 0.5 nm S–S distance, larger than the distance of ~ 0.46 nm, usually quoted for perpendicular alkyl chains in a close-packed layer. On the other hand, thiolate monolayers on Ag(111) are more densely packed owing to the shorter S–S distance. There were a number of different reports on chain tilt in SAMs on Ag(111), probably owing to different amounts of oxide, formed on the clean metallic surface (229, 230, 296, 297). In carefully prepared SAMs of alkanethiolates on a clean Ag(111) surface, the alkyl chains are practically perpendicular to the surface.

Functionalized alkanethiolate SAMs are important both for engineering of surface properties and for further chemical reactions. Simple, eg, CH_3, CF_3, $CH{=}CH_2$, C≡CH, Cl, Br, CN, OH, OCH_3, NH_2, $N(CH_3)_2$, SO_3H, and $Si(OCH_3)_3$, COOH, $COOCH_3$, $CONH_2$ (206–210, 219, 260, 298, 299, 211), as well as more complex functionalities, eg, ferrocenyl (268, 300–307), biotinyl (308–312), 2,2-bipyridyl (313), tetrathiafulvalenecarboxylate (314), tetraphenylporphyrin (315, 316), and ferrocenylazobenzene (317), were attached to the chain termina of alkanethiolate monolayers. These monolayers are thus becoming the system of choice for studies of surface phenomena, electron transfer, molecular recognition, etc.

Surface OH and COOH are very useful groups for chemical transformations. Monolayers having terminal COOH functionality react with alkanoic acids (318), and decylamine (319) to form bilayer H-bonding-stabilized structures, which lack long-term stability owing to the strong electrostatic repulsion in the newly formed charged interface. The caboxylate group can be transformed to the corresponding acid chlorides by using $SOCl_2$ (320). Further reactions with amines and alcohols yield bilayer structures with amide and ester linkages, respectively. Reaction of the acid chloride with a carboxylic acid-terminated thiol provides the corresponding thioester. This reaction has been used to form polymeric self-assembled monolayers and multilayers from the diacetylene $HS(CH_2)_{10}C{\equiv}C{-}C{\equiv}C(CH_2)_{10}COOH$ (321).

SAMs of OH-terminated alkanethiols have been used in many surface modification reactions (Fig. 14). These reacted with OTS to yield a well-ordered bilayer (322), with octadecyldimethylchlorosilane (323, 324), with $POCl_3$ (325–327), with trifluoroacetic anhydride (328), epichlorohydrin (329), with alkylisothiocyanate (330), with glutaric anhydride (331), and with chlorosulfonic acid (327).

2.3. Alkyl Monolayers on Silicon

Robust monolayers can be prepared where the alkyl chains are covalently bound to a silicon substrate mainly by C–Si bonds (332, 333). In the first experiments hydrogen-terminated silicon, H–Si(111) and H–Si(100), were used with diacetylperoxide (332). These monolayers, although exhibiting thickness, wettability, and methylene-stretching frequencies indicative of highly packed chains, lost $\sim 30\%$ of the chains when exposed to boiling water. The apparent conclusion was that hydrolyzable acyloxy groups are removed, leaving the robust alkyl chains bound to the surface by the C–Si bonds. In an attempt to reduce the fraction of surface acyloxy groups, a mixture of alkene and diacetylperoxide was used (333). Reaction of alkynes also yielded robust, closely packed monolayers, and chlorine-terminated olefins gave monolayers having wettability indicative of CI-terminated alkyl chains. The resulting monolayers are $\sim 90\%$ olefin-based, as shown by deuterium labeling experiments.

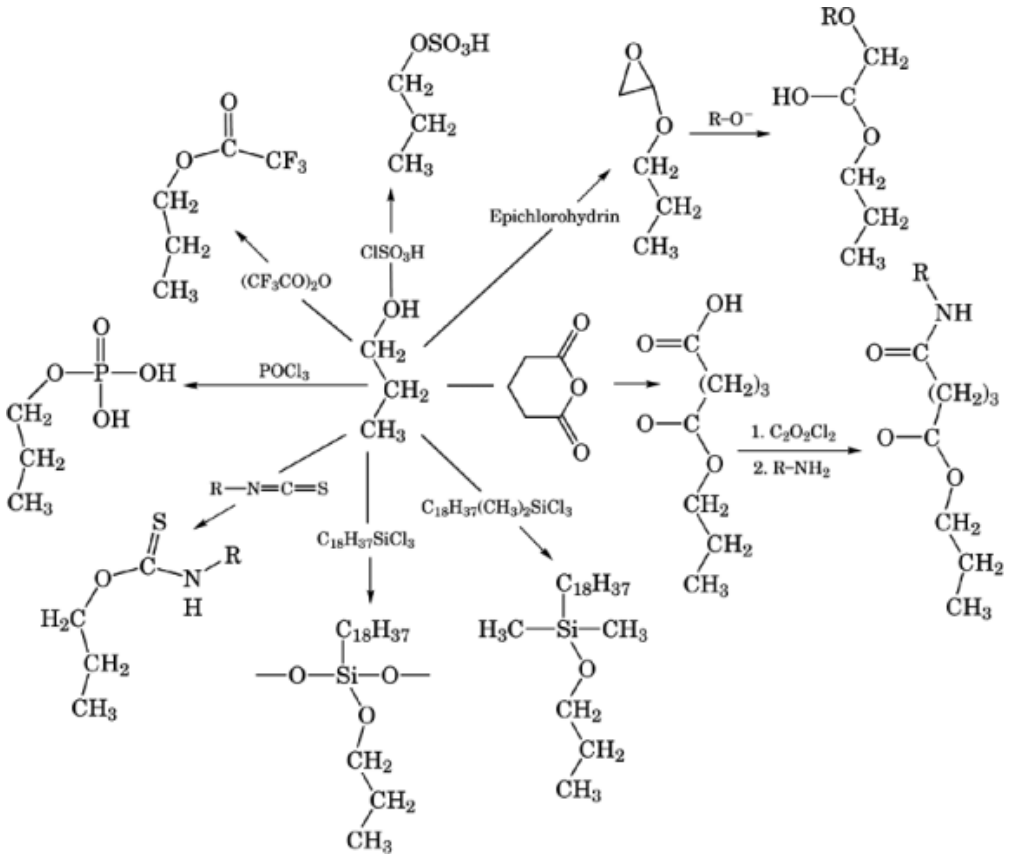

Fig. 14. Surface reactions of ω-hydroxy alkanethiolate monolayers on Au(111).

The introduction of olefin molecules can be explained by a radical reaction. The surface radical (dangling bond $(\cdot)$) reacts with the double-bond to yield a secondary carbon radical:

$$R'CH{=}CH_2 + \cdot Si\,(111) \longrightarrow R'CH\,(\cdot) - CH_2 - Si\,(111)$$

This radical can either abstract another hydrogen from the allylic position of an olefin molecule:

$$R'CH\,(\cdot) - CH_2 - Si\,(111) + R'CH_2CH{=}CH_2 \longrightarrow R'\,(CH_2)_2\,Si\,(111) + R'CH\,(\cdot)\,CH{=}CH_2$$

or with a surface Si–H group:

$$R'CH\,(\cdot) - CH_2 - Si\,(111) + H - Si\,(111) \longrightarrow R'\,(CH_2)_2\,Si\,(111) + \cdot Si\,(111)$$

The monolayer density, as measured by x-ray reflectivity, is only $\sim$90% of the value of a crystalline paraffin such as n-$C_{33}H_{68}$, suggesting a significant number of defects. Ellipsometry and infrared spectroscopy suggest that the chains are tilted $\sim 45^\circ$ from the surface normal, and that a twist angle of $\sim 53^\circ$ exists between the plane that bisects the methylene groups and the plane of the tilt. This tilt angle is not surprising because the interchain distance is 0.665 nm (334).

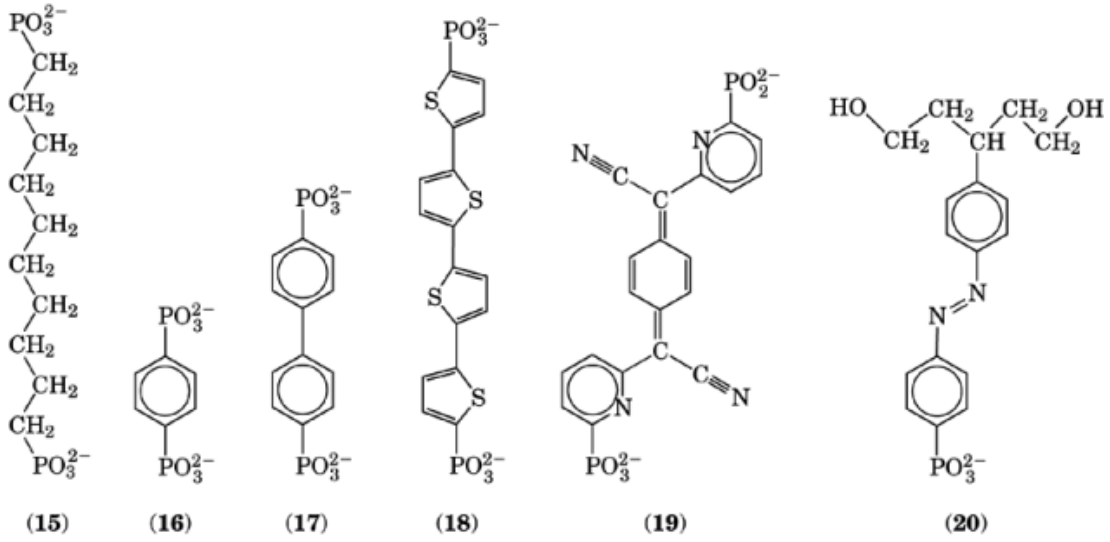

Fig. 15. Diphosphonic acids used in self-assembled multilayer preparation.

Monolayers of alkyl chains on silicon are a significant addition to the family of SAMs. An ability to directly connect organic materials to silicon allows a direct coupling between organic materials and semiconductors. The fine control of superlattice structures provided by the self-assembly technique offers a route for building organic thin films with, for example, electrooptic properties on silicon.

2.4. Multilayers of Diphosphates

One way to find surface reactions that may lead to the formation of SAMs is to look for reactions that result in an insoluble salt. This is the case for phosphate monolayers, based on their highly insoluble salts with tetravalent transition metal ions. In these salts, the phosphates form layer structures, one OH group sticking to either side. Thus, replacing the OH with an alkyl chain to form the alkyl phosphonic acid was expected to result in a bilayer structure with alkyl chains extending from both sides of the metal phosphate sheet (335). When zirconium(IV) is used the distance between next neighbor alkyl chains is ~ 0.53 nm, which forces either chain disorder or chain tilt so that VDW attractive interactions can be reestablished.

Self-assembled multilayers can be prepared simply by alternating adsorption of Zr^{4+} ions and α,ω-alkylidenediphosphate 15 on a phosphorylated surface (336, 337). Other diphosphates have also been investigated (237, 325, 326, 338–340) (Fig. 15). These are all centrosymmetric multilayers.

For second-order NLO applications, the films need to be noncentrosymmetric. 4-Di(2-hydroxyethyl)amino-4′-azobenzenephosphonate was used to form SAMs on zirconium-treated phosphorylated surfaces. Further reaction with $POCl_3$ and hydrolysis created a new phosphorylated surface that could be treated with zirconium salt (341–343). The principal advantage of the phosphate systems is high thermal stability, simple preparation, and the variety of substrates that can be used. The latter is especially important if transparent substrates are required. Thiolate monolayers are not transparent, and alkyltrichlorosilanes have a serious stability disadvantage.

2.5. Surface Engineering Using SAMs

Independent control of surface structure and chemical properties and the resulting structure property relationships are scientifically interesting and technologically important. For many applications, controlling the properties of interfaces is very important. However, in real-life circumstances, interfaces that contain at least one polymer surface are typically irregular. Surface properties of polymers depend critically upon the chemical and physical details of molecular structure at the surface of the polymer. To control surface properties by manipulating surface structure, it is necessary to have an extensive database of detailed correlations between properties and structure for the polymer surface of interest.

Surface properties are generally considered to be controlled by the outermost 0.5–1.0 nm at a polymer film (344). A logical solution, therefore, is to use self-assembled monolayers (SAMs) as model polymer surfaces. To understand fully the breadth of surface interactions, a portfolio of chemical functionalities is needed. SAMs are especially suited for the studies of interfacial phenomena owing to the fine control of surface functional group concentration.

In choosing a SAM system for surface engineering, there are several options. Silane monolayers on hydroxylated surfaces are an option where transparent or nonconductive systems are needed. However, trichlorosilane compounds are moisture-sensitive and polymerize in solution. The resulting polymers contaminate the monolayer surface, which occasionally has to be cleaned mechanically. Carboxylic acids adsorb on metal oxide, eg, Al_2O_3, AgO through acid–base interactions. These are not specific; therefore, it would be impossible to adsorb a carboxylic acid selectively in the presence of, for example, a terminal phosphonic acid group. In many studies SAMs of thiolates on Au(111) are the system of choice.

The structure of SAMs is affected by the size and chemical properties of surface functionalities. Indeed, the introduction of any surface functionality reduces monolayer order. The impetus toward disorder may result from sterically demanding terminal groups, eg, $–O–Si(CH_3)_2(C(CH_3)_3)$ (245) and $–C_5H_5N{:}Ru(NH_3)_5$ (345, 346), or from very polar surface groups, eg, OH, COOH, etc. In both cases, the disorder introduced may be significant and not confined only to the surface.

The sensitivity of wetting to surface chemistry is evident from an OH-concentration-driven wetting transition of hexadecane (Fig. 16) (110), observed in the study of mixed SAMs containing varying proportions of hydrophobic, CH_3, and hydrophilic, OH, components. A mechanism based on the influence of surface-adsorbed water layers was supported by calculations based on a mean-field Cahn-type wetting analysis. These calculations also predicted the correct trend in the transition-onset position as a function of relative humidity (347). As relative humidity decreases, the transition-onset shifts to higher surface OH-concentration. This prediction was confirmed experimentally. In an experiment demonstrating the sensitivity of the wetting process to surface roughness at the molecular level, two CH_2 groups (together, 0.25 nm-long) were added to the hydrophobic component. The wetting transition disappeared, demonstrating the potential of surface engineering using SAMs, where changes at the molecular level made possible by utilizing mixed SAMs may result in control of macroscopic surface properties. The success of surface engineering at the molecular level requires surface stability, ie, that surface functional groups not initiate or promote surface reorganization. Moreover, since it can be expected that structural changes at the surface penetrate into the monolayer bulk, surface stability may have a significant effect on the equilibrium structure of the monolayer. Surface reorganization is a complex phenomenon. It is not clear a priori to what depth conformational changes that start at the surface can penetrate.

Instability in the wettability behavior of OH surfaces was noticed when OH-terminated silane monolayers were exposed to hydrophobic solvents, such as CCl_4 (175). Similarly, monolayers of 11-hydroxyundecane-thiol (HUT), $HO–(CH_2)_{11}–SH$, on Au(111) surfaces have been found to undergo surface reorganization by exposure to ambient atmosphere for a few hours (328). After that, the water contact angle reached a value of ca 60°, and only ca 25% of the OH groups could be esterified by trifluoroacetic anhydride. Molecular dynamics simulations verified that the driving force for the surface reorganization is the formation of surface-correlated H-bonds (348,

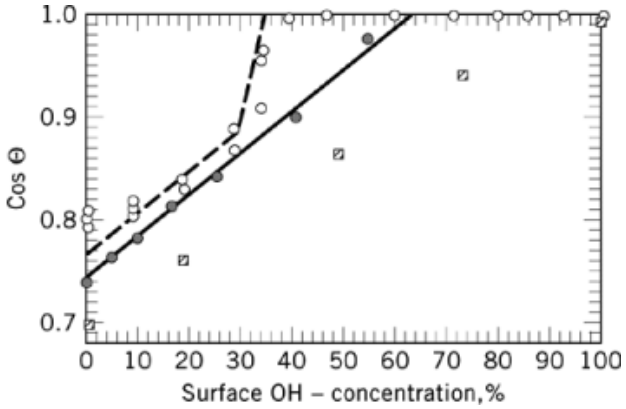

Fig. 16. Cos θ of hexadecane for $HO(CH_2)_{11}SH$ and $CH_3(CH_2)_{11}SH$ in 30% RH (^) and in $\leq$2% RH (●), and for $HO(CH_2)_{11}SH$ and $CH_3(CH_2)_{13}SH$ (▨) mixed alkanethiolate SAMs on gold, as a function of surface OH-concentration. The lines represent theoretical calculations.

349). Surface instability was also observed for mixed monolayers. The decrease of surface-free energy with time increases with the increasing number of surface OH groups, ie, with the increase of surface-free energy. These observations would support the assumption of a mechanism in which surface-free energy decreases owing to the decrease of surface OH groups, resulting from conformational changes at chain termina. As surface-free energy increases, the tendency toward reorganization, which results in exposure of CH_2 groups and a surface energy decrease, increases. This tendency can be offset by strong intermolecular interactions. Stability studies of monolayers made of a longer-chain derivative, $HO–(CH_2)_{21}–SH$, as a function of temperature showed that surface reorganization is indeed a function of monolayer melting point.

Every monolayer surface, even that made of CH_3 groups, is disordered at room temperature because of gauche defects at the chain termina. However, whereas the concentration of surface gauche defects is a function of free volume, the latter is a function of the adsorption scheme and of molecular cross-sectional area. Furthermore, surface reorganization may be augmented by the formation of H-bonds, as in the case of surface OH groups, or be restricted by the size and shape of the functional group, OH, vs COOH, or SO_3H. Temperature, relative humidity, and adsorption at the monolayer surface are other factors that affect surface stability. The equilibrium structure of a surface is the result of balancing all these factors, and is very hard to predict. However, the stability of a monolayer against reorganization may be increased by intermolecular interactions, as described; however, studies confirming this hypothesis have not yet been carried out.

2.6. Conclusions

Future strategies for building supramolecular devices may be based on molecular biology principles. The assembly of modules of increasing hierarchic order and the testing of modules before each assembly step, rejecting incorrect samples has been suggested (Fig. 17). Having such a sequence is a basic requirement for avoiding accumulating more defects when increasing the complexity of the assembly. The naturally occurring mechanism for such self-repair in biosystems is the aggregation of modules. Thus, incorrect samples that do not match are rejected and exchanged for the correct ones.

Beyond the self-organization of two-dimensional assemblies at interfaces, the next level of complexity requires controlling the third dimension. The different fabrication methods for organized molecular films offer a mechanism for building multilayer films, each having its own advantages and disadvantages. Amphiphiles used in the LB technique are reasonably stable, but the resultant films are unstable thermally, with the possible

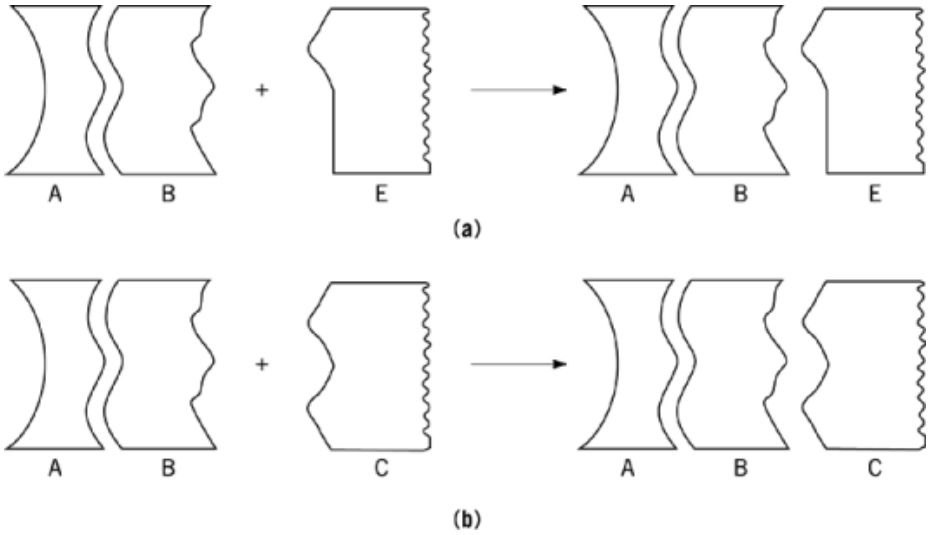

Fig. 17. Testing modules before each assembly step and rejecting incorrect samples: (**a**) E, an erroneous copy, is rejected; whereas (**b**) C, a correct copy, is accepted.

exception of those made of polymeric amphiphiles. In the latter case, however, the viscosity of the layer prevents fast deposition rates and may limit large-scale fabrication of useful devices. Understanding how the structure of a polymeric amphiphile, its molecular weight and molecular weight distribution, relate to the viscosity of its monolayer at the air–water interface is of crucial importance. Relating deposition rates to parameters such as surface viscosity and temperature is not a straightforward matter, and requires a large matrix of experiments. Analyzing the resulting films for defects and relating order parameters to deposition rates is also a complete task. Nevertheless, without such efforts, it is difficult to envision actual utilization of the LB technique in manufacturing.

The advantage of the LB technique is that it allows systematic studies of 2-D organization, both before and after transfer from the air–water interface onto a solid substrate. However, the coupling of 3-D self-organization of macromolecules in solution with organization at a solid surface may best be achieved using the self-assembly technique.

Whereas research in SAMs was originally motivated by a potential for application as building blocks for superlattices having engineered physical properties, the more immediate contribution to science and technology should come from utilization in surface engineering. One example of a potential technology is semiconductor surface patterning. Silane derivatives have been used (350) and the utility of alkanethiol monolayers demonstrated (267, 351). Another important example is transducer technology, where optical piezoelectric, and other forms of chemical sensors have been demonstrated using SAMs (352). In this context, Raman spectroscopy is an attractive means of detection, when coupled with the unique interfacial SAM properties (353). Surfaces of piezoelectric devices have been modified with SAMs (354). There, engineering of donor–acceptor, hydrophilic–hydrophobic, and complexation properties via tailoring chain termina functionalities lead to detection of gaseous analytes (355, 356).

Electroanalytical chemistry is one of the areas where advantage of the unique properties of SAMs is clear, and where excellent advanced analytical strategies can be utilized, especially when coupled with more complex SAM architectures. There are a number of examples where redox reactions are used to detect biomaterials (357, 358), and where guest–host chemistry has been used to exploit specific interactions (356, 359). Ion-selective

electrodes are an application where SAMs may provide new technologies. Selectivity to divalent cations such as Cu^{2+} but not to trivalent ions such as Fe^{3+} has been demonstrated (360).

Future development of SAM-based analytical technology requires expansion of the size and shape selectivity of template structures, as well as introduction of advanced chemical and optical gating mechanisms. An important contribution of SAMs is in miniaturization of analytical instrumentation. This use may in turn have considerable importance in the biomedical analytical area, where miniature analytical probes will be introduced into the body and target-specific organs or even cell clusters. Advances in high resolution spatial patterning of SAMs open the way for such technologies (268, 352).

Another area where contributions can be made using SAMs is in understanding of surface phenomena at the molecular level. For many applications, controlling the properties of interfaces is of primary importance: lubrication of moving parts, manufacture of photographic films, and the interaction of colloidal particles, eg, polymer beads and toner particles in xerography. In such applications, the interface is typically irregular, and the control of structure, chemical functionality, and roughness at the molecular level is practically impossible. Using SAMs allows for the systematic modification of surface-free energy and chemical properties. The trapping of polymer chains near a surface (361) and its dependence on surface functionalities can be investigated. The appearance of slippage at the wall depends on the polymer–wall interaction strength (362), and can also be studied.

The spreading rate of a polymer droplet on a surface has been measured (363, 364). The diffusion constant was at least an order of magnitude smaller than that of the bulk. The monomer–surface friction coefficient for polystyrene has been measured on a number of surfaces and excellent agreement with reptation theory modified to account for increased friction owing to surface–monomer contact obtained (365).

Finally, engineered surfaces may contribute to the understanding of adhesion (172). Control of adhesion is essential to a large number of industrial processes and is often associated with various problems, but currently (ca 1997) there is little if any understanding of how specific molecular ordering and interactions at the surface may affect adhesion.

Surfaces used in adhesion at the engineering level are far from being in a molecularly ordered, well-characterized state. This fact in turn makes it difficult to distinguish the relative degrees of importance among the many different effects that are ultimately responsible for adhesion. The complexity of adhesion phenomena may be addressed by minimizing the number of uncontrolled parameters by using SAMs as model surfaces, thus reducing the ambiguity.

BIBLIOGRAPHY

Cited Publications

1. I. Langmuir, *Trans. Faraday Soc.* **15**, 62 (1920).
2. K. B. Blodgett, *J. Am. Chem. Soc.* **56**, 495 (1934); *idem, ibid.* **57**, 1007 (1935).
3. G. L. Gaines, *Insoluble Monolayers Liquid–Gas Interfaces*; Wiley-Interscience, New York, 1966.
4. A. Ulman, *An Introduction to Ultrathin Organic Films From Langmuir-Blodgett to Self-Assembly*, Academic Press, Boston, 1991.
5. K. B. Blodgett, *Science* **89**, 60 (1939); *idem, Phys. Rev.* **55**, 391 (1939); U.S. Pat. 2,220,861 (1940), K. B. Blodgett (to General Electric Co.).
6. A. W. Adamson, *Physical Chemistry of Surfaces*, John Wiley & Sons, Inc., New York, 1982.
7. M. Lösche, E. Sackmann, and H. Möhwald, *Ber. Bunsenges. Phys. Chem.* **87**, 848 (1983).
8. R. M. Weiss, H. M. McConnell, *Nature* **310**, 5972 (1984).
9. R. Peters and K. Beck, *Proc. Natl. Acad. Sci. USA* **80**, 7183 (1983).

10. B. Moore, C. M. Knohler, D. Broseta, and F. Rondelez, *J. Chem. Soc., Faraday Trans.* **2**, 82 (1986).
11. M. C. Shih, T. M. Bohanon, J. M. Mikrut, P. Zschack, and P. Dutta, *J. Chem. Phys.* **96**, 1556 (1992).
12. For an introduction to liquid crystals see P. J. Collings, *Liquid Crystals Nature's Delicate Phase of Matter*, Princeton Science Library, Princeton, N.J., 1990.
13. S. Ställberg-Stenhagen and E. Stenhagen, *Nature* **156**, 239 (1945).
14. B. Lin, M. C. Shih, T. M. Bohanon, G. E. Ice, and P. Dutta, *Phys. Rev. Lett.* **65**, 191 (1990).
15. A. M. Bibo and I. R. Peterson, *Adv. Mater.* **2**, 309 (1990).
16. K. A. Blodgett and I. Langmuir, *Phys. Rev.* **51**, 964 (1937).
17. K. A. Blodgett, *J. Phys. Chem.* **41**, 975 (1937).
18. K. Fukuda and T. Shiozawa, *Thin Solid Films* **68**, 55 (1980).
19. R. Popovitz-Biro and co-workers, *J. Am. Chem. Soc.* **112**, 2498 (1990).
20. I. Langmuir and V. J. Schaefer, *J. Am. Chem. Soc.* **59**, 1406, 1762 (1937).
21. T. Kato, *Jpn. J. Appl. Phys. Part 2* **27**, L1358 (1988).
22. T. Kato, M. Arai, and K. Ohshima, *Nippon Kagaku Kaishi*, 1774 (1988).
23. H. Kuhn, D. Möbius, H. Bucher, in A. Weissberger, B. W. Rossiter, eds., *Techniques of Chemistry*, John Wiley & Sons, Inc., New York, 1973; Part 3B, Vol. **1**, p. 577ff.
24. P. A. Chollet, *Thin Solid Films* **52**, 343 (1978).
25. J. F. Rabolt, F. C. Burns, N. E. Schlotter, and J. D. Swalen, *J. Chem. Phys.* **78**, 946 (1983).
26. A. Barraud, C. Rosilio, and A. Ruaudel-Teixier, *J. Colloid Interface Sci.* **62**, 509 (1977).
27. A. Barraud and C. Rosilio, *Solid State Technol.* **22**, 120 (1979).
28. A. Barraud, *Thin Solid Films* **99**, 317 (1983).
29. F. Kajzar and J. Messier, *Thin Solid Films* **132**, 11 (1985).
30. H. Kelker and R. Hatz, *Handbook of Liquid Crystals*, Verlag Chemie, Weinheim, Germany, 1980.
31. T. Sakuhara, H. Nakahara, and K. Fukuda, *Thin Solid Films* **159**, 345 (1988).
32. M. J. Cook, M. F. Daniel, K. J. Harrison, N. B. McKeown, and A. J. Thomson, *J. Chem. Soc. Chem. Commun.*, 1148 (1987).
33. N. B. McKeown and co-workers, *Thin Solid Films* **159**, 469 (1988).
34. M. J. Cook, N. B. McKeown, and A. J. Thomson, *Chem. Mater.* **1**, 287 (1989).
35. I. Langmuir and V. J. Shaefer, *J. Am. Chem. Soc.* **59**, 2075 (1937).
36. A. Ruaudel-Teixier, A. Barraud, B. Belbeoch, and M. Roulliay, *Thin Solid Films* **99**, 33 (1983).
37. P. Lesieur, M. Vandevyver, A. Ruaudel-Teixier, and A. Barraud, *Thin Solid Films* **159**, 315 (1988).
38. A. W. Snow and N. L. Jarvis, *J. Am. Chem. Soc.* **106**, 4706 (1984).
39. W. R. Barger, A. W. Snow, H. Wohltjen, and N. L. Jarvis, *Thin Solid Films* **133**, 197 (1985).
40. D. P. Dilella, W. R. Barger, A. W. Snow, and R. R. Smardzewski, *Thin Solid Films* **133**, 207 (1985).
41. A. W. Snow, W. R. Barger, M. Klusky, H. Wohltjen, and N. L. Jarvis, *Langmuir* **2**, 513 (1986).
42. M. D. Pace, W. R. Barger, and A. W. Snow, *J. Mag. Res.* **75**, 73 (1987).
43. W. R. Barger, J. Dote, M. Klusty, R. Mowery, R. Price, and A. W. Snow, *Thin Solid Films* **159**, 369 (1985).
44. J. D. Shutt, D. A. Batzel, R. V. Sudiwala, S. E. Rickert, and M. E. Kenney, *Langmuir* **4**, 1240 (1988).
45. A. Cemel, T. Fort Jr., and J. B. Lando, *J. Polym. Sci. A-1* **10**, 2061 (1972).
46. A. Barraud, C. Rosilio, and A. Ruaudel-Teixier, *Microcircuit Engineering 79*, Institut of Semiconductors and Electronics, Aachen, Germany, 1979, p. 127.
47. H. G. Winful, J. H. Harburger, and E. Garmire, *Appl. Phys. Lett.* **35**, 379 (1979).
48. C. T. Seaton, X. Mau, G. I. Stegeman, and H. G. Winful, *Opt. Eng.* **24**, 593 (1985).
49. D. Sarid, *Opt. Lett.* **6**, 552 (1981).
50. A. Lattes, H. A. Haus, F. J. Leonberger, and E. P. Ipen, *IEEE J. Quant. Elect.* **QE-19**, 1718 (1983).
51. R. J. Leymour and co-workers, *Proc. SPIE* **578**, 137 (1985).
52. B. Tieke, G. Wegner, D. Naegele, and H. Ringsdorf, *Angew. Chem. Int. Ed. Engl.* **15**, 764 (1976).
53. B. Tieke and G. Wegner, in E. Kay and P. S. Bagus, eds., *Topics in Surface Chemistry*, Plenum Press, New York, 1978, p. 121.
54. D. Day and H. Ringsdorf, *J. Polym. Sci., Polym. Lett. Ed.* **16**, 205 (1978).
55. D. Day and H. Ringsdorf, *Makromol. Chem.* **180**, 1059 (1979).
56. D. Day, J. B. Lando, and H. Ringsdorf, *Polym. Prepr., Am. Chem. Soc., Div. Polym. Chem.* **19**, 176 (1978).

57. K. Lochner, H. Bässler, B. Tieke, and G. Wegner, *Phys. Stat. Solidi B* **82**, 633 (1978).
58. G. Wegner, *Z Naturfosch., Teil B* **24**, 824 (1969).
59. G. Wegner, *Pure Appl. Chem.* **49**, 443 (1977).
60. F. Grunfeld and C. W. Pitt, *Thin Solid Films* **99**, 249 (1983).
61. R. H. Tredgold and C. S. Winter, *J. Phys. D* **15**, L55 (1982).
62. H. Ringsdorf, G. Schmidt, and J. Schneider, *Thin Solid Films* **152**, 207 (1987).
63. R. Elbert, A. Laschewsky, and H. Ringsdorf, *J. Am. Chem. Soc.* **107**, 4134 (1985).
64. B. L. Henke, *Adv. X-Ray Anal.* **7**, 460 (1947).
65. G. Roberts, ed., *Langmuir-Blodgett Films*, Plenum Press, New York, 1990.
66. O. A. Aktsipetrov and E. D. Mishina, *JEPT Lett.* **37**, 207 (1983).
67. G. L. Gaines Jr., *Anal. Chem.* **48**, 450 (1976).
68. M. F. Daniel and G. W. Smith, *Mol. Cryst. Liq. Cryst.* **102**, 193 (1984).
69. J. E. Kuder and D. Wychick, *Chem. Phys. Lett.* **102**, 193 (1974).
70. G. L. Gaines Jr., *Nature* **298**, 544 (1982).
71. I. R. Girling, N. A. Cade, P. V. Kolinsky, and C. M. Montgomery, *Elect. Lett.* **21**, 169 (1985).
72. G. W. Smith, M. F. Daniel, J. W. Barton, and N. Ratcliffe, *Thin Solid Films* **132**, 125 (1985).
73. P. Christie, G. G. Roberts, and M. C. Petty, *Appl. Phys. Lett.* **48**, 1101 (1986).
74. M. B. Biddle and S. E. Rickert, *Ferroelectrics* **76**, 133 (1987).
75. H. Kuhn, *J. Photochem.* **10**, 111 (1979).
76. R. A. Marcus, *J. Chem. Phys.* **63**, 2654 (1965).
77. E. E. Polymeropoulos, D. Möbius, and H. Kuhn, *J. Chem. Phys.* **68**, 3918 (1978).
78. *Idem., Thin Solid Films* **68**, 173 (1980).
79. T. Tran-Thi, S. Palacin, and B. Clergeot, *Chem. Phys. Lett.* **157**, 92 (1989).
80. A. Aviram and M. A. Ratner, *Chem. Phys. Lett.* **29**, 277 (1974).
81. A. S. Martin, J. R. Sambles, and G. J. Ashwell, *Thin Solid Films*, **210–211**, 313 (1992).
82. D. J. Sandman and co-workers, *Synth. Met.* **42**, 1415 (1991).
83. N. J. Geddes, J. R. Sambles, D. J. Jarvis, W. G. Parker, and D. Sandman, *J. Appl. Phys. Lett.* **56**, 1916 (1990).
84. M. Fujihira, in A. Ulman, ed., *Thin Films*, Vol. **20**, Academic Press, Boston, 1995.
85. G. G. Roberts, K. P. Pande, and W. A. Barlow, *Proc. IEE Part 1* **2**, 169 (1978).
86. M. C. Petty and G. G. Roberts, in G. G. Roberts, ed., *Proc. INFOS 79*, Institute of Physics, London, 1980, p. 186.
87. K. K. Kan, M. C. Petty, and G. G. Roberts, *Thin Solid Films* **99**, 291 (1983).
88. J. P. Lloyd, M. C. Petty, G. G. Roberts, P. G. LeComber, and W. E. Spear, *Thin Solid Films* **89**, 4 (1982).
89. J. P. Lloyd, M. C. Petty, G. G. Roberts, P. G. LeComber, and W. E. Spear, *Thin Solid Films* **89**, 2974 (1982).
90. G. G. Roberts, K. P. Pande, and W. A. Barlow, *Electron. Lett.* **13**, 581 (1977).
91. H. Raether, *Phys. Thin Films* **9**, 145 (1977).
92. J. P. Lloyd, C. Pearson, and M. C. Petty, *Thin Solid Films* **160**, 431 (1988).
93. R. B. Beswick and C. W. Pitt, *J. Colloid Interface Sci.* **124**, 146 (1988).
94. R. B. Beswick and C. W. Pitt, *Chem. Phys. Lett.* **143**, 589 (1988).
95. B. Holcroft and G. G. Roberts, *Thin Solid Films* **160**, 445 (1988).
96. T. Moriizumi, *Thin Solid Films* **160**, 413 (1988).
97. W. M. Reichert, C. J. Bruckner, and J. Joseph, *Thin Solid Films* **152**, 345 (1987).
98. A. Arya, U. J. Krull, M. Thompson, and H. E. Wong, *Anal. Chim. Acta* **173**, 331 (1985).
99. J. Anzai, K. Furuya, C. Chen, T. Osa, and T. Matsuo, *Anal. Sci.* **3**, 271 (1987).
100. J. Anzai, J. Hashinoto, T. Osa, and T. Matsuo, *Anal. Sci.* **4**, 247 (1988).
101. H. Tsuzuki and co-workers, *Chem. Lett.*, 1265 (1988).
102. M. Sriyudthsak, H. Yamagishi, and T. Moriizumi, *Thin Solid Films* **160**, 463 (1988).
103. Y. Okahata, T. Tsuruta, K. Ijiro, and K. Ariga, *Langmuir* **4**, 1373 (1988).
104. M. Aizawa, M. Matsuzawa, and H. Shinohara, *Thin Solid Films* **160**, 477 (1988).
105. J. Anzai, S. Lee, T. Osa, and T. Makromol, *Chem., Rapid Commun.* **10**, 167 (1989).
106. H. Kuhn and A. Ulman, in Ref. 86, pp.
107. W. C. Bigelow, D. L. Pickett, and W. A. Zisman, *J. Colloid Interface Sci.*, **1**, 513 (1946).
108. R. G. Nuzzo and D. L. Allara, *J. Am. Chem. Soc.* **105**, 4481 (1983).

109. P. Ball, *Designing the Molecular World*, Princeton University Press, Princeton, N.J., 1994.
110. A. Ulman, S. D. Evans, Y. Shnidman, R. Sharma, J. E. Eilers, and J. C. Chang, *J. Am. Chem. Soc.* **113**, 1499 (1991).
111. A. Kumar, H. A. Biebuyck, and G. M. Whitesides, *Langmuir* **10**, 1498 (1994).
112. D. A. Tirrell, *MRS Bulletin*, (July 23–28, 1991).
113. D. L. Allara and R. G. Nuzzo, *Langmuir* **1**, 45 (1985).
114. *Ibid.*, 52.
115. H. Ogawa, T. Chihera, and K. Taya, *J. Am. Chem. Soc.* **107**, 1365 (1985).
116. N. E. Schlotter, M. D. Porter, T. B. Bright, and D. L. Allara, *Chem. Phys. Lett.* **132**, 93 (1986).
117. D. Y. Huang and Y.-T. Tao, *Bull. Inst. Chem., Acad. Sin.* **33**, 73 (1986).
118. Y. Shnidman, A. Ulman, and J. E. Eilers, *Langmuir* **9**, 1071 (1993).
119. M. G. Samart, C. A. Brown, and J. G. Gordon, *Langmuir* **9**, 1082 (1993).
120. Y.-T. Tao, *J. Am. Chem. Soc.* **115**, 4350 (1993).
121. W. R. Thompson and J. E. Pemberton, *Langmuir* **11**, 1720 (1995).
122. E. L. Smith and M. D. Porter, *J. Phys. Chem.* **97**, 4421 (1993).
123. A. H. M. Soundag, A. J. W. Tol, and F. J. Touwslager, *Langmuir* **8**, 1127 (1992).
124. Y.-T. Tao, M.-T. Lee, and S.-C. Chang, *J. Am. Chem. Soc.* **115**, 9547 (1993).
125. J. Sagiv, *J. Am. Chem. Soc.* **102**, 92 (1980).
126. P. Silberzan, L. Léger, D. Ausserré, and J. J. Benattar, *Langmuir* **7**, 1647 (1991).
127. S. R. Wasserman, Y.-T. Tao, and G. M. Whitesides, *Langmuir* **5**, 1074 (1989).
128. J. D. Le Grange, J. L. Markham, and C. R. Kurjian, *Langmuir* **9**, 1749 (1993).
129. R. Maoz and J. Sagiv, *J. Colloid and Interf. Sci.* **100**, 465 (1984).
130. J. Gun and J. Sagiv, *J. Colloid and Interf. Sci.* **112**, 457 (1986).
131. J. Gun, R. Iscovici, and J. Sagiv, *J. Colloid and Interf. Sci.* **101**, 201 (1984).
132. N. Tillman, A. Ulman, and J. S. Schildkraut, and T. L. Penner, *J. Am. Chem. Soc.* **110**, 6136 (1988).
133. S. Brandriss and S. Margel, *Langmuir* **9**, 1232 (1993).
134. K. Mathauser and C. W. Frank, *Langmuir* **9**, 3002 (1993).
135. K. Mathauser and C. W. Frank, *Langmuir* **9**, 3446 (1993).
136. G. Carson and S. Granick, *J. Appl. Polym. Sci.* **37**, 2767 (1989).
137. C. R. Kessel and S. Granick, *Langmuir* **7**, 532 (1991).
138. D. K. Schwartz, S. Steinberg, J. Israelachvili, and Z. A. N. Zasadzinski, *Phys. Rev. Lett.* **69**, 3354 (1992).
139. H. O. Finklea and co-workers, *Langmuir* **2**, 239 (1986).
140. I. Rubinstein, E. Sabatani, R. Maoz, and J. Sagiv, *Proc. Electrochem. Soc.* **86**, 175 (1986).
141. I. Rubinstein, E. Sabatani, R. Maoz, and J. Sagiv, *Electroanal. Chem.* **219**, 365 (1987).
142. D. L. Allara, A. N. Parikh, and F. Rondelez, *Langmuir* **11**, 2357 (1995).
143. C. P. Tripp and M. L. Hair, *Langmuir* **8**, 1120 (1992).
144. D. L. Angst and G. W. Simmons, *Langmuir* **7**, 2236 (1991).
145. M. E. McGovern, K. M. R. Kallury, and M. Thompson, *Langmuir* **10**, 3607 (1994).
146. S. R. Wasserman and co-workers, *J. Am. Chem. Soc.* **111**, 5852 (1989).
147. C. P. Tripp and M. L. Hair, *Langmuir* **11**, 149 (1995).
148. W. Gao and L. Reven, *Langmuir* **11**, 1860 (1995).
149. K. Bierbaum and co-workers, *Langmuir* **11**, 512 (1995).
150. R. Banga, J. Yarwood, A. M. Morgan, B. Evans, and J. Kells, *Langmuir* **11**, 4393 (1995).
151. S. R. Cohen, R. Naaman, and J. Sagiv, *J. Chem. Phys.* **90**, 3054 (1986).
152. T. Ohtake, N. Mino, and K. Ogawa, *Langmuir* **8**, 2081 (1992).
153. I. M. Tidswell and co-workers, *Phys. Rev.* **B41**, 1111 (1990).
154. T. Nakagawa and K. Ogawa, *Langmuir* **10**, 367 (1994).
155. H. Okusa, K. Kurihara, and T. Kunitake, *Langmuir* **10**, 8 (1994).
156. M. Fujii, S. Sugisawa, K. Fukada, T. Kato, T. Shirakawa, and T. Seimiya, *Langmuir* **10**, 984 (1994).
157. N. Yoshino, *Chem. Lett.*, 735 (1994).
158. K. Bierbaum and M. Grunze, *Adhesion Soc.*, 213 (1994).
159. D. H. Flinn, D. A. Guzonas, and R.-H. Yoon, *Colloids Surf. A.* **87**, 163 (1994).
160. Y.-I. Rabinovich and R.-H. Yoon, *Langmuir* **10**, 1903 (1994).

161. C. A. Siedlecki, S. L. Eppell, and R. E. Marchant, *J. Biomed. Mater. Res.* **28**, 271 (1994).
162. K. Mathauer and C. W. Frank, *Langmuir* **9**, 3446 (1993).
163. L. Netzer, R. Iscovichi, and J. Sagiv, *Thin Solid Films* **100**, 67 (1983).
164. M. Pomerantz, A. Segmüller, L. Netzer, and J. Sagiv, *Thin Solid Films*, **132**, 153 (1985).
165. N. Tillman, A. Ulman, and T. L. Penner, *Langmuir* **5**, 101 (1989).
166. D. G. Kurth and T. Bein, *Langmuir* **11**, 2965 (1995).
167. *Ibid.*, 3061.
168. C. N. Durfor, D. C. Turner, J. H. Georger, B. M. Peek, and D. A. Stenger, *Langmuir* **10**, 148 (1994).
169. J. Lühe, V. J. Novotny, K. K. Kanazawa, T. Clarke, and G. B. Street, *Langmuir* **9**, 2383 (1993).
170. X.-D. Xiao, G.-Y. Liu, D. H. Charych, and M. Salmeron, *Langmuir* **11**, 1600 (1995).
171. X.-D. Xiao, J. Hue, D. H. Charych, and M. Salmeron, *Langmuir* **12**, 235 (1996).
172. M. K. Chaudhury and G. M. Whitesides, *Science* **255**, 1230 (1992).
173. N. Balachander and C. N. Sukenik, *Langmuir* **6**, 1621 (1990).
174. Y. W. Lee, J. Reed-Mundell, C. N. Sukenik, and J. E. Zull, *Langmuir* **9**, 3009 (1993).
175. J. A. Chupa and co-workers, *J. Am. Chem. Soc.* **115**, 4383 (1993).
176. S. Paulson, K. Morris, and B. P. Sullivan, *J. Chem. Soc. Chem. Commun.*, 1615 (1992).
177. S. R. Wasserman, H. Biebuyck, and G. M. Whitesides, *J. Mater. Res.* **4**, 886 (1989).
178. M. Maoz and J. Sagiv, *Langmuir* **3**, 1034 (1987).
179. M. Maoz and J. Sagiv, *Langmuir* **3**, 1045 (1987).
180. R. Maoz, L. Netzer, J. Gun, and J. Sagive, *J. Chim. Phys. (Paris)* **85**, 1059 (1988).
181. L. Netzer and R. Iscovici, J. Sagiv, *Thin Solid Films* **99**, 235 (1983).
182. R. Netzer and J. Sagiv, *J. Am. Chem. Soc.* **105**, 674 (1983).
183. R. Maoz and J. Sagiv, *Thin Solid Films* **132**, 135 (1985)K.
184. Ogawa, N. Mino, H. Tamura, and M. Hatada, *Langmuir* **6**, 851 (1990).
185. *Ibid.*, 1807.
186. D. Q. Li, M. A. Ratner, T. J. Marks, C. H. Zhang, J. Yang, and G. K. Wong, *J. Am. Chem. Soc.* **112**, 7389 (1990).
187. A. K. Kakkar and co-workers, *Langmuir* **9**, 388 (1993).
188. S. Yitzchaik and co-workers, *J. Phys. Chem.* **97**, 6958 (1993).
189. S. B. Roscoe, S. Yitzchaik, A. K. Kakkar, T. J. Marks, W. L. Lin, and G. K. Wong, *Langmuir* **10**, 1337 (1994).
190. C. P. Tripp, R. P. N. Veregin, and M. L. Hair, *Langmuir* **9**, 3518 (1993).
191. (to be supplied)
192. L. J. Jeon, R. G. Nuzzo, Y. Xia, M. Mrksich, and G. M. Whitesides, *Langmuir* **11**, 3024 (1995).
193. Y. Xia, M. Mrksich, E. Kim, and G. M. Whitesides, *J. Am. Chem. Soc.* **117**, 9576 (1995).
194. W. J. Dressick, C. S. Dulcey, J. H. Georger, and J. M. Calvert, *Chem. Mater.* **5**, 148 (1993).
195. K. Chen, W. B. Caldwell, and C. A. Mirkin, *J. Am. Chem. Soc.* **115**, 1193 (1993).
196. D. Q. Li and B. I. Swanson, *Langmuir* **9**, 3341 (1993).
197. V. V. Tsukruk, L. M. Lander, and W. L. Brittain, *Langmuir* **10**, 996 (1994).
198. H.-H. Hong, M. Jiang, S. G. Slinger, and P. Bohn, *Langmuir* **10**, 153 (1994).
199. D. A. Offord and J. H. Griffin, *Langmuir* **9**, 3015 (1993).
200. C. N. Sukenik, personal communication.
201. K. Robinson, A. Ulman, J. Lando, and A. J. Mann, personal communication.
202. T. J. Marks, preprint.
203. R. Maoz, R. Yam, G. Berkovic, and J. Sagiv, in Ref. 86, pp.
204. R. Maoz, J. Sagiv, D. Degenhardt, H. Möhwald, and P. Quint, *Supramol. Sci.* **2**, 9 (1995).
205. N. Mino, K. Ogawa, M. Hatada, M. Takastuka, S. Sha, and T. Moriizumi, *Langmuir* **9**, 1280 (1993).
206. L. H. Dubois and R. G. Nuzzo, *Ann. Phys. Chem.* **43**, 437 (1992).
207. C. D. Bain and G. M. Whitesides, *Adv. Mater.* **1**, 506 (1989).
208. J. P. Folkers, J. A. Zerkowski, P. E. Laibinis, C. T. Seto, and G. M. Whitesides, in T. Bain, ed., *Supramolecular Architecture, ACS Symposium Series 499*, American Chemical Society, Washington, D.C., 1992, 10–23.
209. T. R. Lee, P. E. Laibinis, J. P. Folkers, and G. M. Whitesides, *Pure & Appl. Chem.* **63**, 821 (1991).
210. G. M. Whitesides and G. S. Ferguson, *Chemtracts-Organic Chemistry* **1**, 171 (1988).
211. H. Sellers, A. Ulman, Y. Shnidman, and J. E. Eilers, *J. Am. Chem. Soc.* **115**, 9389 (1993).

212. E. B. Troughton, C. D. Bain, G. M. Whitesides, D. L. Allara, and M. D. Porter, *Langmuir* **4**, 365 (1988).
213. E. Katz, N. Itzhak, and I. Willner, *J. Electroanal. Chem.* **336**, 357 (1992).
214. E. Sabatani, J. Cohen-Boulakia, M. Bruening, and I. Rubinstein, *Langmuir* **9**, 2974 (1993).
215. M. A. Bryant, S. L. Joa, and J. E. Pemberton, *Langmuir* **9**, 753 (1992).
216. W. Hill and B. Wehling, *J. Phys. Chem.* **97**, 9451 (1993).
217. T. T.-T. Li, H. Y. Liu, and M. J. Weaver, *J. Am. Chem. Soc.* **106**, 1233 (1984).
218. J. M. Cooper, K. R. Greenough, and C. J. McNeil, *J. Electroanal. Chem.* **347**, 267 (1993).
219. A. Ihs, K. Uvdal, and B. Liedberg, *Langmuir* **9**, 733 (1993).
220. Th. Arndt, H. Schupp, and W. Schepp, *Thin Solid Films* **178**, 319 (1989).
221. J. A. Mielczarski and R. H. Yoon, *Langmuir* **7**, 101 (1991).
222. T. R. G. Edwards, V. J. Cunnane, R. Parsons, and D. Gani, *J. Chem. Soc. Chem. Commun.*, 1041 (1989).
223. A. J. Arduengo, J. R. Moran, J. Rodriguez-Paradu, and M. D. Ward, *J. Am. Chem. Soc.* **112**, 6153 (1990).
224. G. Xue, X.-Y. Huang, J. Dong, and J. Zhang, *J. Electroanal. Chem.* **310**, 139 (1991).
225. S. Bharathi, V. Yegnaraman, and G. P. Rao, *Langmuir* **9**, 1614 (1993).
226. M. G. Samanat, C. A. Broen, and J. G. Gordon, *Langmuir* **8**, 1615 (1992).
227. G. A. Somorjai, *Chemistry in Two Dimensions—Surfaces*, Cornell University Press, Ithaca, N.Y., 1982.
228. D. E. King, *J. Vac. Sci. Technol.* (1995).
229. A. Ulman, *J. Mater. Educ.* **11**, 205 (1989).
230. P. E. Laibinis and co-workers, *J. Am. Chem. Soc.* **113**, 7152 (1991).
231. M. W. Walczak, C. Chung, S. M. Stole, C. A. Widrig, and M. D. Porter, *J. Am. Chem. Soc.* **113**, 2370 (1991).
232. P. E. Laibinis and G. M. Whitesides, *J. Am. Chem. Soc.* **112**, 1990 (1992).
233. A. Ihs and B. Liedberg, *Langmuir* **10**, 734 (1994).
234. P. E. Laibinis and G. M. Whitesides, *J. Am. Chem. Soc.* **114**, 9022 (1992).
235. K. Shimazu, Y. Sato, I. Yagi, and K. Uosaki, *Bull. Chem. Soc. Jpn.* **67**, 863 (1994).
236. A. Demoz and D. J. Harrison, *Langmuir* **9**, 1046 (1993).
237. N. Muskal, I. Turyan, A. Shurky, and D. Mandler, *J. Am. Chem. Soc.* **117**, 1147 (1995).
238. M. Stratmann, *Adv. Mater.* **2**, 191 (1990).
239. M. Volmer, M. Stratmann, and H. Viefhaus, *Surf. and Interf. Anal.* **16**, 278 (1990).
240. Q. Liu and Z. Xu, *Langmuir* **11**, 4617 (1995).
241. M. Brust, M. Walker, D. Bethell, D. J. Schiffrin, and R. Whyman, *J. Chem. Soc. Chem. Commun.*, 801 (1994).
242. C. W. Sheen, J. X. Shi, J. Martensson, A. N. Parikh, and D. L. Allara, *J. Am. Chem. Soc.* **114**, 1514 (1992).
243. Y. Gu, B. Lin, V. S. Smentkowski, and D. H. Waldeck, *Langmuir* **11**, 1849 (1995).
244. A. Ulman, personal communication.
245. C. D. Bain and co-workers, *J. Am. Chem. Soc.* **111**, 321 (1989).
246. M. Buck, F. Eisert, J. Fischer, M. Grunze, and F. Träger, *Appl. Phys.* **A53**, 552 (1991).
247. M. Buck, F. Eisert, and M. Grunze, *Ber. Bunsenges. Phys. Chem.* **97**, 399 (1993).
248. G. Hähner, Ch. Wöll, M. Buck, and M. Grunze, *Langmuir* **9**, 1955 (1993).
249. S. D. Evans, E. Urankar, A. Ulman, and N. J. Ferris, *J. Am. Chem. Soc.* **113**, 4121 (1991).
250. D. A. Offord, C. M. John, M. R. Linford, and J. H. Griffin, *Langmuir* **10**, 883 (1994).
251. H. A. Biebuyck, C. D. Bain, and G. M. Whitesides, *Langmuir* **10**, 1825 (1994).
252. H. A. Biebuyck and G. M. Whitesides, *Langmuir* **9**, 1766 (1993).
253. N. Mohri, M. Inoue, Y. Arai, and K. Yoshikawa, *Langmuir* **11**, 1612 (1995).
254. P. Fenter, A. Eberhardt, and P. Eisenberger, *Science* **266**, 1216 (1994).
255. R. C. Thomas, L. Sun, and M. Crooks, *Langmuir* **7**, 620 (1991).
256. O. Chailapakul, L. Sun, C. Xu, and M. Crooks, *J. Am. Chem. Soc.* **115**, 12459 (1993).
257. M. D. Porter, T. B. Bright, D. L. Allara, and C. E. D. Chidsey, *J. Am. Chem. Soc.* **109**, 3559 (1987).
258. R. G. Nuzzo, F. A. Fusco, and D. L. Allara, *J. Am. Chem. Soc.* **109**, 2358 (1987).
259. C. D. Bain, H. A. Biebuyck, and G. M. Whitesides, *Langmuir* **5**, 723 (1989).
260. R. G. Nuzzo, B. R. Zegarski, and L. H. Dubois, *J. Am. Chem. Soc.* **109**, 733 (1987).
261. R. G. Nuzzo, L. H. Dubois, and D. L. Allara, *J. Am. Chem. Soc.* **112**, 558 (1990).
262. Y. Li, J. Huang, R. T. McIver Jr., and J. C. Hemminger, *J. Am. Chem. Soc.* **114**, 2428 (1992).
263. C. A. Widrig, C. Chung, and M. D. Porter, *J. Electroanal. Chem.*, (1991).

264. M. A. Bryant and J. E. Pemberton, *J. Am. Chem. Soc.* **113**, 3630 (1991).
265. *Ibid.*, 8284.
266. J. B. Schlenoff, M. Li, and H. Ly, *J. Am. Chem. Soc.* **117**, 12528 (1995).
267. J. J. Hickman, D. Ofer, C. Zou, M. S. Wrighton, P. E. Laibinis, and G. M. Whitesides, *J. Am. Chem. Soc.* **113**, 1128 (1991).
268. D. M. Collard and M. A. Fox, *Langmuir* **7**, 1192 (1991).
269. K. A. Groat and S. E. Creager, *Langmuir* **9**, 3668 (1993).
270. M. S. Ravenscroft and H. O. Finklea, *J. Phys. Chem.* **98**, 3843 (1994).
271. L. S. Curtin and co-workers, *Anal. Chem.* **65**, 368 (1993).
272. D. M. Jaffey and R. J. Madix, *J. Am. Chem. Soc.* **116**, 3012 (1994).
273. L. Strong and G. M. Whitesides, *Langmuir* **4**, 546 (1988).
274. C. E. D. Chidsey and D. N. Loiacono, *Langmuir* **6**, 709 (1990).
275. L. H. Dubois, B. R. Zegarski, and R. G. Nuzzo, *J. Chem. Phys.* **98**, 678 (1993).
276. C. E. D. Chidsey, G.-Y. Liu, Y. P. Rowntree, and G. Scoles, *J. Chem. Phys.* **91**, 4421 (1989).
277. C. A. Alves, E. L. Smith, and M. D. Porter, *J. Am. Chem. Soc.* **114**, 1222 (1992).
278. G. E. Poirier, M. J. Tarlov, and H. E. Rushneier, *Langmuir* **10**, 3383 (1994).
279. P. Fenter, P. Eisenberger, and K. S. Liang, *Phys. Rev. Lett.* **70**, 2447 (1993).
280. N. Camillone, C. E. D. Chidsey, G.-Y. Liu, and G. Scoles, *J. Phys. Chem.* **98**, 3503 (1993).
281. G. E. Poirier and M. J. Tarlov, *Langmuir* **10**, 2859 (1994).
282. G. Edinger, A. Gölzhäuser, K. Demota, Ch. Wöll, and M. Grunze, *Langmuir* **9**, 4 (1993).
283. C. Schönenberger, J. A. M. Sondag-Huethorst, J. Jorritsma, and L. G. J. Fokkink, *Langmuir* **10**, 611 (1994).
284. M. Grunze, *Phys. Scripta*, 0000, (1993).
285. R. L. McCarley, D. J. Dunaway, and R. J. Willicut, *Langmuir* **9**, 2775 (1993).
286. J.-P. Bucher, L. Santesson, and K. Kern, *Langmuir* **10**, 979 (1994).
287. K. Schwaha, N. D. Spencer, and R. M. Lambert, *Surf. Sci.* **81**, 273 (1979).
288. G. Rovida and F. Pratesi, *Surf. Sci.* **104**, 609 (1981).
289. A. L. Harris, C. E. D. Chidsey, N. J. Levinos, and D. N. Loiacono, *Chem. Phys. Lett.* **141**, 350 (1987).
290. A. L. Harris, L. Rothberg, L. Dhar, N. J. Levinos, and L. H. Dubois, *J. Phys. Chem.* **94**, 2438 (1991).
291. T. Seto, T. Hara, and K. Tanaka, *Jpn. J. Appl. Phys.* **7**, 31 (1968).
292. P. Fenter and co-workers, *Langmuir* **7**, 2013 (1991).
293. A. Dhirani, M. A. Hines, A. J. Fisher, O. Ismail, and P. Guyot-Sionnest, *Langmuir* **11**, 2609 (1995).
294. J. Y. Gui, D. A. Stern, D. G. Frank, F. Lu, D. C. Zapien, and A. T. Hubbard, *Langmuir* **7**, 955 (1991).
295. J. Y. Gui, F. Lu, D. A. Stern, and A. T. Hubbard, *J. Electroanal. Chem.* **292**, 245 (1990).
296. A. Nemetz, T. Fischer, A. Ulman, and W. Knoll, *J. Chem. Phys.* **98**, 5912 (1993).
297. P. Fenter and P. Eisenberger, personal communication.
298. C. E. D. Chidsey and D. N. Loiacono, *Langmuir* **6**, 682 (1990).
299. K. Dohlhofer, J. Figura, and J.-H. Fuhrhop, *Langmuir* **8**, 1811 (1992).
300. C. E. D. Chidsey, C. R. Bertozzi, T. M. Putvinski, and A. M. Mujsce, *J. Am. Chem. Soc.* **112**, 4301 (1990).
301. K. Uosaki, Y. Sata, and H. Kita, *Langmuir* **7**, 1510 (1991).
302. C. E. D. Chidsey, *Science* **251**, 919 (1991).
303. D. D. Popenoe, R. S. Deinhammer, and M. D. Porter, *Langmuir* **8**, 2521 (1992).
304. Y. Sato, B. L. Frey, R. M. Corn, and K. Uosaki, *Bull. Chem. Soc. Jpn.* **67**, 21 (1994).
305. S. E. Creager and G. K. Rowe, *Anal. Chim.* **246**, 233 (1991).
306. G. K. Rowe and S. E. Creager, *Langmuir* **7**, 2307 (1991).
307. G. K. Rowe and S. E. Creager, *Langmuir* **10**, 1186 (1994).
308. L. Häussling, H. Ringsdorf, F.-J. Schmitt, and W. Knoll, *Langmuir* **7**, 1837 (1991).
309. L. Häussling, B. Michel, H. Ringsdorf, and H. Rohrer, *Angew. Chem. Int. Ed. Engl.* **30**, 679 (1991).
310. F.-J. Schmitt, L. Häussling, H. Ringsdorf, and W. Knoll, *Thin Solid Films* **210/211**, 815 (1992).
311. J. Spinke, J. Liley, H.-J. Guder, L. Angermaier, and W. Knoll, *Langmuir* **9**, 1821 (1993).
312. J. Spinke, M. Liley, F.-J. Schmitt, H.-J. Guder, L. Angemaier, and W. Knoll, *J. Chem. Phys.* **99**, 7012 (1993).
313. Y. S. Obeng and A. J. Bard, *Langmuir* **7**, 195 (1991).
314. C. M. Yip and M. D. Ward, *Langmuir* **10**, 549 (1994).

315. J. Zak, H. Yuan, K. Woo, and M. D. Porter, *Langmuir* **9**, 2772 (1993).
316. J. E. Hutchinson, T. A. Postlethwaite, and R. W. Murray, *Langmuir* **9**, 3277 (1993).
317. B. R. Herr and C. A. Mirkin, *J. Am. Chem. Soc.* **116**, 1157 (1994).
318. L. Sun, J. Kepley, and R. M. Crooks, *Langmuir* **8**, 2101 (1992).
319. L. Sun, R. M. Crooks, and A. J. Ricco, *Langmuir* **9**, 1775 (1993).
320. R. V. Duevel and R. M. Corn, *Anal. Chem.* **64**, 337 (1992).
321. T. Kim, R. M. Crooks, M. Tsen, and L. Sun, preprint.
322. A. Ulman and N. Tillman, *Langmuir* **5**, 1418 (1989).
323. L. Sun, R. C. Thomas, R. M. Crooks, and A. J. Ricco, *J. Am. Chem. Soc.* **113**, 8550 (1991).
324. C. Xu, L. Sun, L. J. Kepley, and R. M. Crooks, *Anal. Chem.* **65**, 2102 (1993).
325. M. L. Schilling and co-workers, *Langmuir* **9**, 2156 (1993).
326. S. F. Bent, M. L. Schilling, W. L. Wilson, H. E. Katz, and A. L. Harris, *Chem. Mater.* **6**, 122 (1994).
327. L. Bertilsson and B. Liedberg, *Langmuir* **9**, 141 (1993).
328. S. D. Evans, R. Sharma, and A. Ulman, *Langmuir* **7**, 156 (1991).
329. S. Löfs and B. Johnsson, *J. Chem. Soc. Chem. Commun.*, 1526 (1990).
330. I. Wilner, A. Riklin, B. Shoham, D. Rivenson, and E. Katz, *Adv. Mater.* **5**, 912 (1993).
331. H. Keller, W. Schrepp, and H. Fuchs, *Thin Solid Films* **210/211**, 799 (1992).
332. M. R. Linford and C. E. D. Chidsey, *J. Am. Chem. Soc.* **115**, 12631 (1993).
333. M. R. Linford, C. E. D. Chidsey, P. Fenter, and P. M. Eisenberger, *J. Am. Chem. Soc.* **116** (1995).
334. A. Ulman, J. E. Eilers, and N. Tillman, *Langmuir* **5**, 1147 (1989).
335. G. Cao, H.-G. Hong, and T. E. Mallouk, *Acc. Chem. Res.* **25**, 420 (1992).
336. H. Lee, L. J. Kepley, H.-G. Hong, and T. E. Mallouk, *J. Am. Chem. Soc.* **110**, 618 (1988).
337. H. Lee, L. J. Kepley, H.-G. Hong, S. Akhter, and T. E. Mallouk, *J. Phys. Chem.* **92**, 2597 (1988).
338. H. E. Katz, M. L. Schilling, S. B. Ungahse, T. M. Putvinski, and C. E. D. Chidsey, in T. Bein, ed., *Supramolecular Architecture, ACS Symposium Series 499*, American Chemical Society: Washington, D.C., 1992, 24–32.
339. H. E. Katz, M. L. Schilling, C. E. D. Chidsey, T. M. Putvinski, and R. S. Hutton, *Chem. Mater.* **3**, 699 (1991).
340. S. B. Ungahse, W. L. Wilson, H. E. Katz, R. G. Scheller, and T. M. Putvinski, *J. Am. Chem. Soc.* **114**, 8717 (1992).
341. T. M. Putvinski, M. L. Schilling, H. E. Katz, C. E. D. Chidsey, A. M. Mujsce, and A. B. Emerson, *Langmuir* **6**, 1567 (1990).
342. H. E. Katz, R. G. Scheller, T. M. Putvinski, M. L. Schilling, W. L. Wilson, and C. E. D. Chidsey, *Science* **254**, 1485 (1991).
343. H. E. Katz and M. L. Schilling, *Chem. Mater.* **5**, 1162 (1993).
344. D. L. Allara, in W. J. Feast, H. S. Munro, and R. W. Richards, eds., *Polymer Surfaces and Interfaces*, Vol. **II**, John Wiley & Sons, Ltd., Chichester, U.K., 1993, p. 27.
345. H. O. Finklea and D. D. Hanshew, *J. Am. Chem. Soc.* **114**, 3173 (1992).
346. H. O. Finklea and D. D. Hanshew, *J. Electroanal. Chem.* **347**, 327 (1993).
347. D. J. Olbris, A. Ulman, and Y. Shnidman, *J. Chem. Phys.* **102**, 6865 (1995).
348. J. Hautman and M. L. Klein, *Phys. Rev. Lett.* **67**, 1763 (1991).
349. J. Hautman, J. P. Bareman, W. Mar, and M. L. Klein, *J. Chem. Soc. Faraday Trans.* **87**, 2031 (1991).
350. S. J. Potochnik, P. E. Pehrsson, D. S. Y. Hsu, and J. M. Calvert, *Langmuir* **11**, 1842 (1995), and references therein.
351. A. Kumar, N. L. Abbott, E. Kim, H. A. Biebuyck, and G. M. Whitesides, *Acc. Chem. Res.* **28**, 219 (1995).
352. T. E. Mallouk and D. J. Harrison, eds., *Interfacial Design and Chemical Sensing, ACS Symposium Series 561*, American Chemical Society, Washington, D.C., 1994.
353. K. T. Carron, L. Pelterson, and M. Lewis, *Environ. Sci. Technol.* **26**, 1950 (1992).
354. L. J. Kepley, R. M. Crooks, and A. J. Ricco, *Anal. Chem.* **64**, 3191 (1992).
355. K. D. Schierbaum, T. Weiss, J. F. J. Thoden van Velzen, D. N. Reinhoudt, and W. Goepel, *Science* **265**, 1413 (1994).
356. C. M. Duan and M. E. Meyerhoff, *Anal. Chem.* **66**, 1369 (1994).
357. Y. Kajiya, T. Okamoto, and H. Yoneyama, *Chem. Lett.* **12**, 2107 (1993).
358. C. Chung and M. D. Porter, *Chem. Eng. News* 32 (May 1, 1989).
359. M. T. Rojas, R. Koniger, J. F. Stoddart, and A. E. Kaifer, *J. Am. Chem. Soc.* **117**, 336 (1995).
360. S. Steinberg, Y. Tor, E. Sabatani, and I. Rubinstein, *J. Am. Chem. Soc.* **113**, 5176 (1991).

361. P. G. deGennes, in J. Charvolin, J. F. Joanny, and J. Zinn-Justin, eds., *Conference Proceedings, Liquids at Interfaces*, Les Houches 1990, North Holland, Amsterdam, 1990.
362. E. Manias, G. Hadziioannou, I. Bitsanis, and G. ten Brinke, *Europhys. Lett.*, 1996, in press.
363. P. Silberzan and L. Leger, *Macromolecules* **25**, 1267 (1992).
364. V. J. Novotny, *J. Chem. Phys.*, 3189 (1990).
365. X. Zheng and co-workers, *Phys. Rev. Lett.* **74**, 407 (1995).

ABRAHAM ULMAN
Polytechnic University

Related Articles

Molecular modeling; Liquid crystalline materials